行政院國家科學委員會專題研究計畫 期中進度報告

以奈米現場效應電晶體及光學感測器探討神經網路功能--1.奈米線場效電晶體及偵測生物系統之應用 2.以量子點探討神經分泌膠囊的新陳代謝機制(總計畫暨子計畫一)(2/3)
期中進度報告(精簡版)

計 畫 類 別 ： 整合型
計 畫 編 號 ： NSC 95-2627-M-002-003-
執 行 期 間 ： 95 年 08 月 01 日至 96 年 10 月 31 日
執 行 單 位 ： 國立臺灣大學化學系暨研究所

計 畫 主 持 人 ： 陳逸聰
共 同 主 持 人 ： 潘建源

報 告 附 件 ： 出席國際會議研究心得報告及發表論文

處 理 方 式 ： 本計畫可公開查詢

中 華 民 國 96 年 07 月 16 日

行政院國家科學委員會補助專題研究計畫
成果報告

計畫名稱：以奈米線場效電晶體及光學感測器探討神經網路功能

計畫類別： □個別型計畫　　■ 整合型計畫
計畫編號： NSC 95-2627-M-002-003
執行期間： 95 年 8 月 1 日至 96 年 7 月 31 日

計畫主持人：陳逸聰 教授
共同主持人：潘建源 助理教授
計畫參與人員：

蔡佳璋（博士後研究員），廖國棠（博士後研究員），賴俊陽（博士後研究員），王建惟（助理），吳智陽（助理），吳幸臻（博士生），李長琪（碩士生），江佩玲（碩士生），于書翰（碩士生）。

成果報告類型：■精簡報告　□完整報告

本成果報告包括以下應繳交之附件：
□赴國外出差或研習心得報告一份
□赴大陸地區出差或研習心得報告一份
□出席國際學術會議心得報告及發表之論文各一份
□國際合作研究計畫國外研究報告書一份

執行單位：國立臺灣大學化學系暨研究所

中　華　民　國　96　年　5　月　16　日

In the past year, we have accomplished two research studies in (a) In-situ detection of chromogranin A released from living neurons with single-walled carbon nanotube field-effect transistor s and (b) Lysophospholipids regulate the cellular excitability and exocytosis in cultured bovine chromaffin cells.

In the in-situ detection of cellular excitability and exocytosis with nanotube/nanowire field-effect transistors, we have demonstrated that single-walled carbon nanotube field effect transistors (SWCNT-FETs) can be used to monitor the synaptic transmissions among primary cultured embryonic cortical neurons. Chromogranin A (CgA) is one of the molecules released from the secretory vesicles when the vesicles are fused with plasma membrane. The expression of CgA has been identified in neuron and neuroendocrine cells. It has been reported that the appearance of CgA in plasma is an excellent marker for neuroendocrine tumors and neurodegenerative diseases like Parkinson's and Alzheimer's diseases. Therefore, the detection of CgA is an indicator of synaptic activity when synaptic vesicle at the presynaptic terminal is triggered to undergo exocytosis. In this study, we have demonstrated that CgA released from the synaptic terminal of living neurons can be detected directly with high selectivity and sensitivity by the CgA-antibody modified SWCNT-FETs. This novel sensory technique of SWCNT-FETs is promising in medical examination and can further be applied to study the activity of an individual neuron cell which should open a new window to enlighten the neurophysiology in neuronal network.

This work has been accepted for publication: "In-situ detection of chromogranin A released from living neurons with single-walled carbon nanotube field-effect transistor", C.-W. Wang, C.-Y. Pan, H.-C. Wu, P.-Y. Shih, C.-C. Tsai, K.-T. Liao, L.-L. Lu, W.-H. Hsieh, C.-D. Chen, and Y.-T. Chen; *Small*, **3**, 000-000 (2007).

In the study of lysophospholipids regulating the cellular excitability and exocytosis in cultured bovine chromaffin cells, bioactive lysophospholipids (LPLs) released by blood cells can be used to modulate many cellular activities such as angiogenesis and cell survival. In our study, the effects of sphingosine-1-phosphate (S1P) and lysophosphatidic acid (LPA) on excitability and exocytosis in bovine chromaffin cells were investigated using the whole-cell configuration of the patch-clamp. Voltage-gated Ca^{2+} current was inhibited by S1P and LPA pretreatment in a concentration-dependent manner with IC_{50}s of 0.46 and 0.79 μM, respectively. Inhibition was mostly reversible upon washout and prevented by suramin, an inhibitor of G-protein signaling. Na^{+} current was inhibited by S1P, but not by LPA. However, recovery of Na^{+} channels from inactivation was slowed by both LPLs. The outward K^{+} current was also significantly reduced by both LPLs. Chromaffin cells fired repetitive action potentials in response to minimal injections of depolarizing current. Repetitive activity was dramatically reduced by LPLs. Consistent with the reduction in Ca^{2+} current, exocytosis elicited by a train of depolarizations and the ensuing endocytosis were both inhibited by LPL pretreatments. These data demonstrate the interaction between immune and endocrine systems mediated by the inhibitory effects of LPLs on the excitability of adrenal chromaffin cells.

This work has been accepted for publication: "Lysophospholipids regulate the cellular excitability and exocytosis in cultured bovine chromaffin cells", C.-Y. Pan, A.-Z. Wu, and Y.-T. Chen; *Journal of Neurochemistry*, **100**, 000-000 (2007).

In-Situ Detection of Chromogranin A Released from Living Neurons with Single-Walled Carbon Nanotube Field-Effect Transistor

1. Introduction

Nanotubes or nanowires based field effect transistors (NT/NW-FETs) as biosensors have recently drawn more and more attention in biological research because of their selectivity, sensitivity, and real-time detection capabilities. For biological studies, several one-dimensional semiconducting materials have been applied as sensing elements to construct NT/NW-FETs, such as silicon nanowires,[1] carbon nanotubes,[2~6] and indium oxide nanowires,[7] for a variety of successful detections of proteins,[1~5] nucleic acids,[6,8] cancer markers,[9] and viruses.[10] In particular, Lieber's group recently applied silicon NW-FETs to monitor the electrical signals from single mammalian neurons, where each nanoscale nanowire-axon junction was used for spatially resolved, highly sensitive detection, stimulation, and/or inhibition of neuronal signal propagation.[11] Their elegant non-invasive measurements of the rate, amplitude, and shape of signals propagating along individual axons and dendrites from the use of silicon NW-FETs have opened a new avenue to the study of neurosciences.

Chromogranin A (CgA), a protein with calculated molecular weight ~50 kDa (apparent molecular weight is 74~80 kDa), is one of the molecules released from secretory vesicles when fused with plasma membrane. CgA plays many important biofunctions, e.g. as an innate immunity to fight against bacterial infection,[12] as a mediator for neuron inflammation,[13] and as a Ca^{2+} chelator to modulate the secretion of other functional biomolecules[14] and to mediate neuronal apoptosis.[15] It has also been reported that the appearance of CgA in plasma is an excellent marker for the diagnosis of neuroendocrine tumors and neurodegenerative diseases like Parkinson's and Alzheimer's diseases.[16] Therefore, the detection of CgA can be an indicator of synaptic activity when exocytosis occurs at the presynaptic terminal and a diagnostic tool for clininic examination. In the past year, we chose single-walled carbon nanotubes (SWCNTs) to configure FETs on account of their high biocompatibility for neuron cells[17] and their sensitive detection capability of the CgA released from living cells. The experimental results show that the SWCNT-FETs are a promising biosensor to monitor the in-situ release of CgA during synaptic transmission among primary cultured embryonic cortical neurons and can be used as a new tool to examine the synaptic activity.

2. Results and Discussion

2.1. Preparation of SWCNT-FET biosensors

A schematic illustration of SWCNT-FET biosensors is shown in Figure 1. The FET

devices were fabricated following a standard photolithographic procedure. After the fabrication of outer electrodes (represented in white color in Figure 1a) with Au/Cr (50/50 nm in thickness), SWCNTs of 2 nm in diameter (Thomas Swan Co. & Ltd.) were transferred to a SiO_2/Si substrate (400 nm thick SiO_2) by dip-coating the substrate in the solution containing SWCNTs

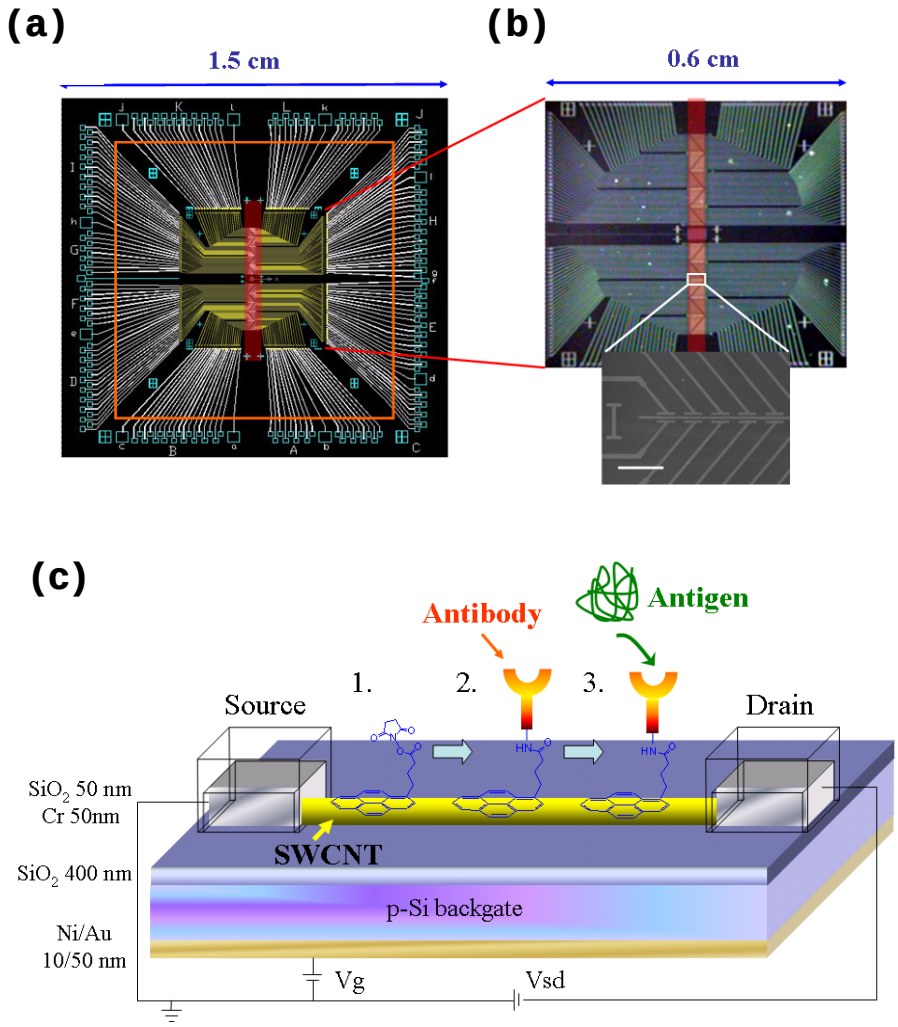

Figure 1. (a) The mask design for the photolithographic fabrications of SWCNT-FET device array. (b) The device array on magnified scales. (upper) An optical image for the circuits in the yellow square area and (lower) the SEM image of an SWCNT-FET array with the source-drain separation of 2 μm. The scale bar is 50 μm (c) Schematic illustration of an SWCNT-FET sensor for the source (Cr, 50 nm in thickness), drain (Cr, 50 nm), and backgate (Ni/Au, 10/50 nm) electrodes on a SiO_2 (400 nm)/Si substrate. The source and drain electrodes were further passivated with an insulating layer of SiO_2 (50 nm) to avoid electric leakage to sample solution. The schematic also shows the immobilization and molecular recognition procedures: 1. The adsorption of linkers onto the SWCNT through a π-π interaction. 2. The immobilization of antibody. 3. The detection of antigen by antibody.

and 0.125% sodium dodecylbenzene sulfonate (NaDDBS) as a surfactant following the method developed by Islam et al.[18] After baking at 200°C for 12 hr to remove the NaDDBS,[19] the as-dispersed SWCNTs in the central area (the reddish rectangles in Figures 1a~b) were electrically contacted by 50 nm thick Cr leads (represented in yellow color in Figure 1a) which were further passivated with a layer of 50 nm thick SiO_2 by thermal evaporation to avoid electric leakage to sample solution. The original pattern design and photolithographic fabrication for this kind of device array by Lieber's group can be found in Refs. 10, 11, and 20. Ni/Au (10/50 nm in thickness) layers coated to the bottom of the SiO_2/Si substrate were used as a backgate.

The as-fabricated SWCNT-FETs were then conversed to functional sensors by immobilizing the complementary probes, which will later be used against target molecules, onto the surfaces of SWCNTs (Figure 1c). In our experiment, a goat IgG antibody against CgA, denoted as CgA-Ab (Santa Cruz Inc.), served as the probe and was immobilized to the sensing

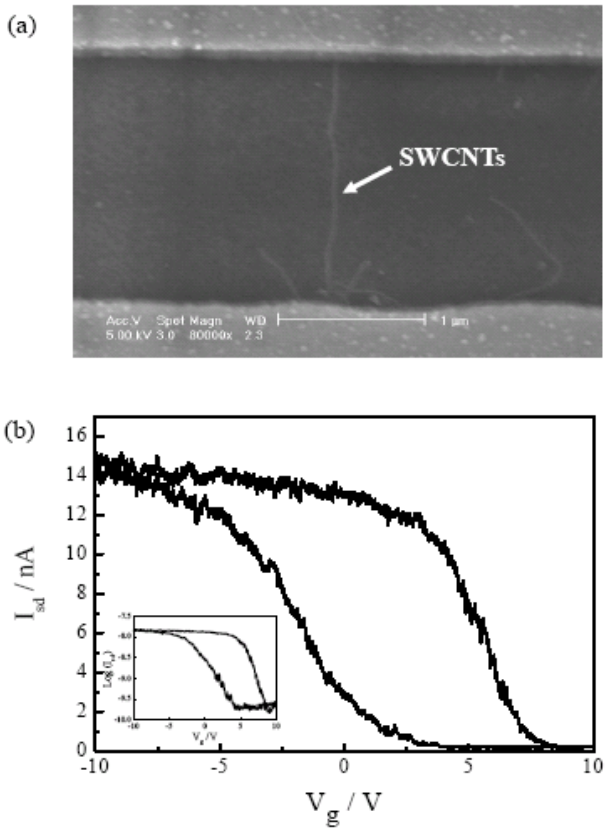

Figure 2. (a) Representative SEM image of an SWCNT-FET device consisting of a pair of source and drain electrodes connected by a small bundle of SWCNTs. (b) A typical I_{sd}-V_g plot for the SWCNT-FET device measured in the ambient air. The inset presents the same data but in a semi-log plot. I_{sd} was measured at V_{sd} = 10 mV and V_g was swept in a negative-positive-negative direction.

devices of SWCNT-FETs with a literature-reported procedure developed by Dai's group.[21,22] After 1-pyrenebutanoic acid succinimidyl ester was applied as a linker to connect antibody with SWCNTs, tween 20 was further used to block nonspecific bindings.

Figure 2a shows the representative scanning electron microscopic (SEM) image for a pair of source and drain electrodes connected by a bundle of SWCNTs. The electrical transporting property of the SWCNT-FET was characterized in the ambient air by measuring the source-drain current vs. backgate voltage (I_{sd}-V_g) curves swept in a negative-positive-negative voltage direction as illustrated in Figure 2b. The current decreases with increasing gate voltage, indicating that the SWCNTs are of p-type. Avouris and co-workers have pointed out that the CNT-FET operation mode is dominated by the Schottky barrier, and the hole-transporting property is mainly due to the oxygen adsorption on the metal-SWCNT junction which causes

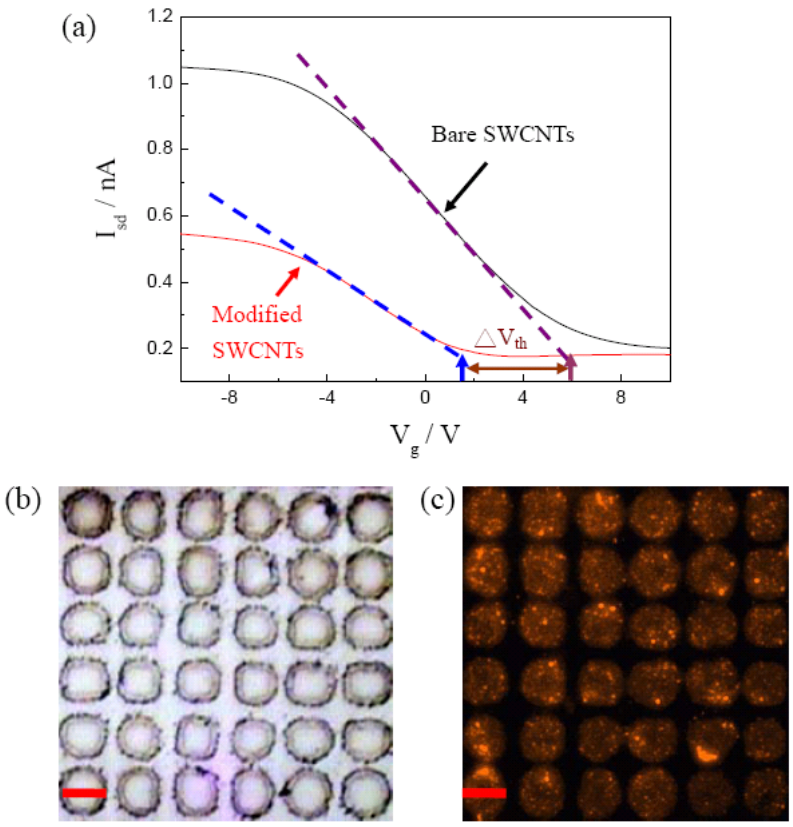

Figure 3. (a) The I_{sd}-V_g curves measured in the ambient air before and after the immobilization of CgA-Ab on an SWCNT-FET. I_{sd} was measured at V_{sd} = 10 mV. The change of threshold voltages (ΔV_{th}) before and after the immobilization of CgA-Ab is indicated. (b) An optical image of the SWCNTs located in the patterned spots fabricated photolithographically. The scale bar is 30 μm. (c) A fluorescence image of the SWCNTs modified with CgA which was further labeled with rhodamine-conjugated rabbit anti-goat IgG antibody. The procedures for the immobilization of CgA-Ab on SWCNTs are described in the context. The scale bar is 30 μm.

the Fermi level of metal to approach the valence band edge of SWCNTs.[23,24] Moreover, the hysteresis in SWCNT-FETs is attributed to the adsorption of water molecules on SWCNTs as discussed by Dai and co-workers.[25]

The immobilization of CgA-Ab onto SWCNTs was demonstrated by two methods: electrical characterization (Figure 3a) and fluorescence microscopy (Figures 3b~c). Figure 3a depicts the I_{sd}-V_g curves, measured in the ambient air, before and after the immobilization of CgA-Ab onto SWCNTs. The shift of threshold-voltage (ΔV_{th}) toward the more negative side indicates an electron donation from the as-immobilized CgA-Ab to SWCNTs due to the electron-donating amino groups of antibodies.[3] In addition, the decrease of current (I_{sd}) after the immobilization of CgA-Ab is also attributed to the effect of potential scattering to reduce the mobility of charge carriers.[3] These observations have indicated the functionalization of CgA-Ab onto SWCNTs. In the fluorescence imaging experiment to characterize the functionalization of CgA-Ab onto SWCNTs, densely matted SWCNTs were first stuffed by repeatedly coating them into prefabricated 10 μm-deep photoresist wells made by a photolithographic technique. After lifting off the photoresist, SWCNT films were left in the patterned spots (Figure 3b). The CgA-Ab was then immobilized onto these SWCNTs with the procedures described earlier. Subsequently, the CgA-Ab modified SWCNTs were incubated with rhodamine-conjugated anti-goat IgG antibody (Santa Cruz Inc.). In Figure 3c, the fluorescence image clearly displays the successful immobilization of CgA-Ab onto the surfaces of SWCNTs.

2.2. Molecular recognition of CgAP by CgA-Ab

The SWCNT-FETs which have been modified with CgA-Ab on the surfaces of SWCNTs will be represented as CgA-Ab/SWCNT-FETs hereafter. To examine the detection efficacy of CgA-Ab/SWCNT-FETs, a peptide that encodes the amino acids 158~457 of CgA (denoted as CgAP, Santa Cruz Inc.) was used. To deliver the CgAP solution onto the CgA-Ab/SWCNT-FETs, a polydimethyl-siloxane (PDMS) microfluidic channel[26] ($6.25\times0.5\times0.05$ mm^3) was designed to couple with the device arrays (the reddish rectangles in Figures 1a~b) and the CgAP sample solution was driven into the channel by a syringe pump. Figure 4a shows the current (I_{sd}) of a CgA-Ab/SWCNT-FET in response to different concentrations of CgAP in PBS (phosphate buffer saline, 137 mM NaCl, 2.7 mM KCl, 10 mM Na_2HPO_4, 2 mM KH_2PO_4, pH 7.4 with NaOH). After balanced with PBS, the I_{sd} was ~1.085 nA in the beginning and showed no significant change in electric conductance when 60 μg/mL bovine serum albumin (BSA) reached the CgA-Ab/SWCNT-FET sensor, manifesting the binding specificity of CgA-Ab. The I_{sd} increased to ~1.093 nA, when 1 nM CgAP was introduced. The I_{sd} moved further up to ~1.13 nA, when CgAP was increased to 10 nM. This sensory device, however, did not respond in proportion to the addition of 100 nM CgAP, indicating a saturation of the binding sites on the CgA-Ab/SWCNT-FET. The sensitive electric

responses have demonstrated the high affinity between CgAP and CgA-Ab/SWCNT-FET. For CgA, a typical isoelectric point (pI) ranges 4.5 ~ 5,[16] and a pI value of 4.49 for the CgAP sequence used in this experiment was provided by the manufacturer. In view of its low pI value, CgAP should be negatively charged in PBS at pH = 7.4. Accordingly, the binding of CgAP onto CgA-Ab/SWCNT-FET should have increased the carrier (hole) concentration, thus enhancing the electric conductivity in the p-type semiconductor device due to a gating effect.

To further investigate the applicability of CgA-Ab/SWCNT-FETs in medical diagnosis, CgAP was dissolved in FBS (fetal bovine serum, JRH Biosciences Inc.) which was aseptically collected via cardiac puncture followed by centrifugation and filtration to remove most blood corpuscles. Unlike PBS, composed of only simple ionic salts (e.g. K^+, Na^+, etc.), FBS contains a variety of proteins and small biomolecules. Therefore, the detection of CgAP in FBS is a

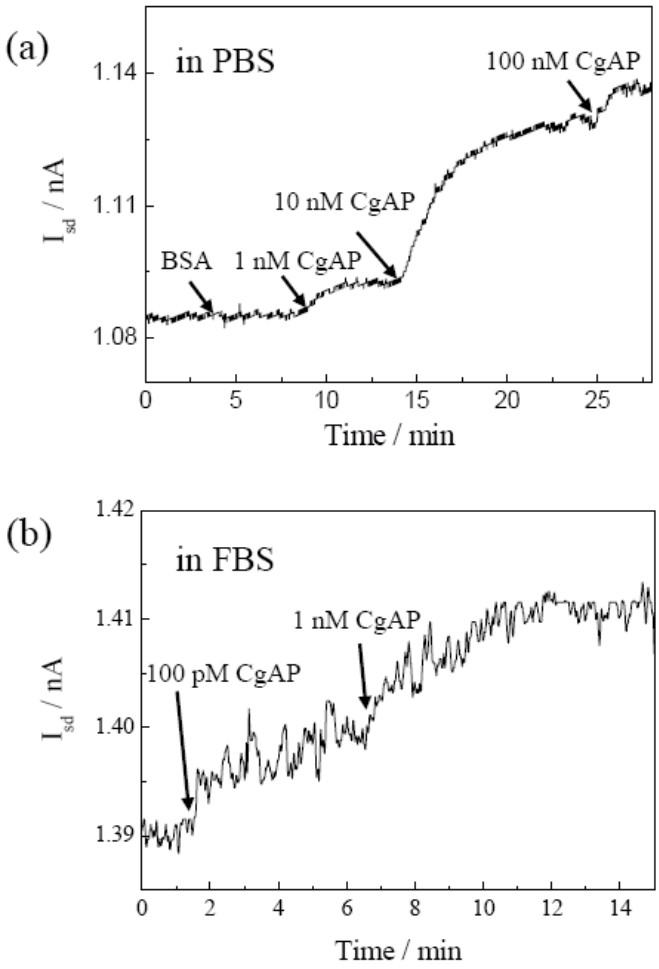

Figure 4. Electric responses of a CgA-Ab/SWCNT-FET to CgAP of different concentrations measured in ambient conditions of (a) PBS and (b) FBS. At the beginning, 60 μg/mL BSA was used as a negative control. Different concentrations of CgAP were then flowed into the PDMS microfluidic channel coupled with the device arrays. I_{sd} was measured at V_{sd} = 10 mV with modulation frequency of 17.7 Hz in both experiments.

stringent test for the diagnostic performance of CgA-Ab/SWCNT-FETs. Figure 4b shows the current responses of a CgA-Ab/SWCNT-FET in the detection of CgAP in FBS with I_{sd} increasing from ~1.390 to ~1.397 nA as 100 pM CgAP reached the device, and further increasing to ~1.41 nA when 1 nM CgAP was added. These results demonstrate that the CgA-Ab/SWCNT-FETs are capable of detecting CgA selectively even at a very low concentration level (≥1 nM) in the complex FBS environment (total protein content ranging from 30 to 45 mg/mL). This capability ensures that the sensitive and selective

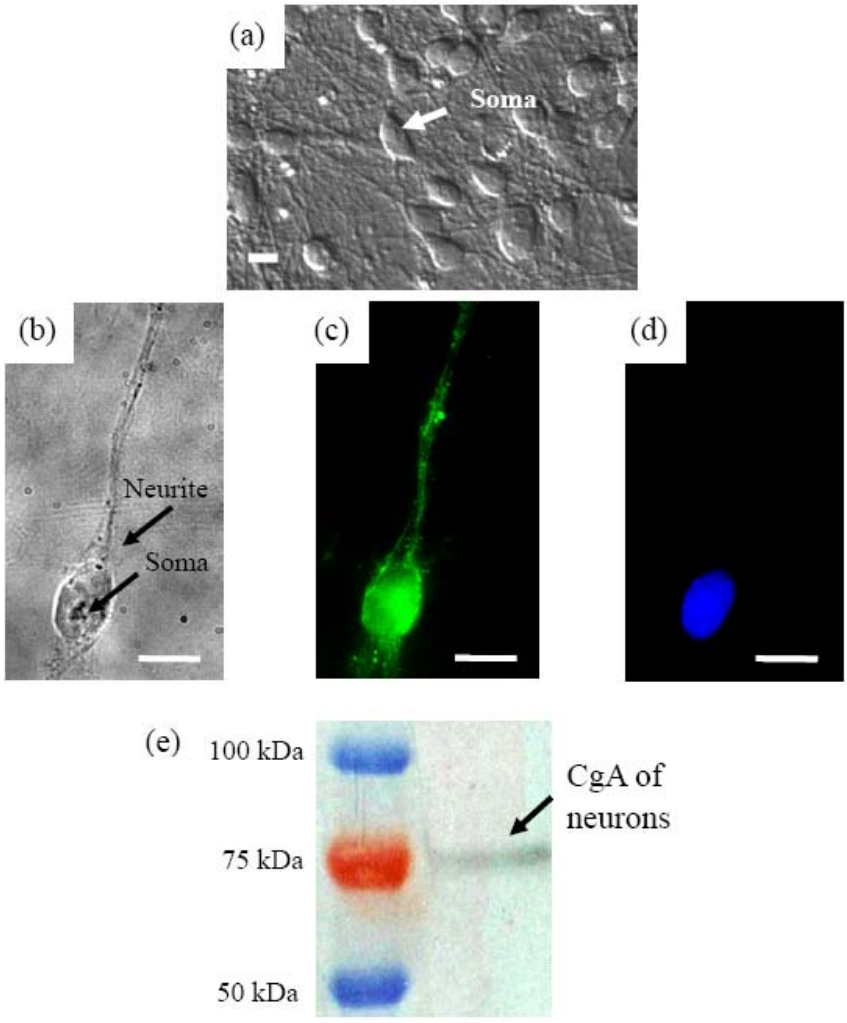

Figure 5. CgA can be detected in cultured cortical neurons. (a) A differential interference contrast microscopic image of live cultured neurons grown on a coverslip. The scale bar is 10 μm. To label both CgA and nucleus in neurons, cells were fixed and stained with the antibody against CgA and DAPI, respectively. The (b) bright field, (c) CgA immunostaining, and (d) nucleus immunostaining images of a single neuronal cell are presented. The scale bars are 10 μm. (e) The cultured neurons were harvested and the total proteins were used for a Western blot experiment. The positions of molecular weight markers (left lane) and CgA from neuron lysate (right lane) are indicated.

CgA-Ab/SWCNT-FETs are suitable for neuronal and neuroendocrine cancer diagnosis.[27] More importantly, these sensory devices have the merits of label-free and real-time detection capabilities in medical applications.

2.3. In-situ detection of CgA released from living neuron

E14.5 cortical neurons were isolated from the embryos of Sprageu-Dawley rat and cultured on a poly-L-lysine pretreated coverslip with the standard protocol as described before.[28] Neurons were used after 7~11 days in culture for the following experiments. The optical image of such cultured neurons is shown in Figure 5a. The cell bodies (somata) are ~10 μm in diameter and the silk-like neurites can be clearly identified. To verify the existence and distribution of CgA in neurons, traditional immunochemistry was performed. Figures 5b~d display the resultant immunostaining images, where single neuronal cells were first immobilized by formalin (4%), and then treated with triton X-100 (0.5%) to permeabilize the cells[29] and with BSA (1%) to avoid nonspecific binding. The endogenous CgA was then stained by the same primary antibody as that was used in modifying the SWCNT-FET device. After rinse, fluorescin isothiocyanate conjugated rabbit anti-goat IgG was used as the secondary antibody (1:2000, diluted with PBS at pH 7.4) to obtain fluorescence image. The nucleus was also stained by diamidino-2-phenylindole (DAPI) which binds selectively to the DNA double helix (Figure 5c). The distribution of green dots indicates that the localization of CgA was in both the cell body and neurites. To further examine the existence of CgA in neurons, the proteins were extracted from cultured neurons and separated by an 8% SDS-PAGE. The proteins on the gel were electrically transferred to a nitrocellulose paper and the antibody against CgA was used to stain the position of CgA. The resultant Western blot examination is depicted in Figure 5e, in which a single band at ~75 kDa was identified, referring to the apparent existence of CgA. The shift of the molecular weight of CgA (~50 kDa) may be due to the denaturing condition used in this experiment as reported by the antibody manufacturer (Santa Cruz Inc.).

A schematic illustration of the in-situ detection of CgA released from neurons by a CgA-Ab/SWCNT-FET is shown in Figure 6a. Glutamate, one of the most common neurotransmitters in brain, was used to stimulate the neurons. The binding of glutamate to the ionotropic glutamate receptors allows Na^+ fluxes into the cytosol and depolarizes the cell. The subsequent opening of the voltage-gated Ca^{2+} channels at the synaptic terminal triggers exocytosis to release CgA, which can then be detected by the CgA-Ab/SWCNT-FET. In the following experiments, instead of using a PDMS microfluidic channel, a plastic wall (located on the orange square in Figure 1a) of 3 mm in height was glued onto the SiO_2/Si chip to hold the normal saline buffer (145 mM NaCl, 5 mM glucose, 10 mM Na-HEPES, 1 mM $MgCl_2$, 5 mM KCl, and 2.2 mM $CaCl_2$, pH 7.3 with NaOH) as illustrated in the cartoon of Figure 6c. The FET electrodes between the orange square and reddish rectangle area of Figure 1a were further

protected by coating a layer of photoresist to prevent them from contacting ionic solution. Before the neuron experiment, a negative control without neurons on the FET device was performed by adding 50 μM glutamate to the CgA-Ab/SWCNT-FET which had been immersed in 100 μL normal saline buffer. No I_{sd} change could be detected (Figure 6b), when glutamate was added. To detect the CgA released from neurons, a piece of coverslip blanketed with cortical neurons was pushed onto the FET chip and incubated in 100 μL normal saline buffer (the cartoon inset of Figure 6c). Care was taken to let neurons face the CgA-Ab/SWCNT-FET.

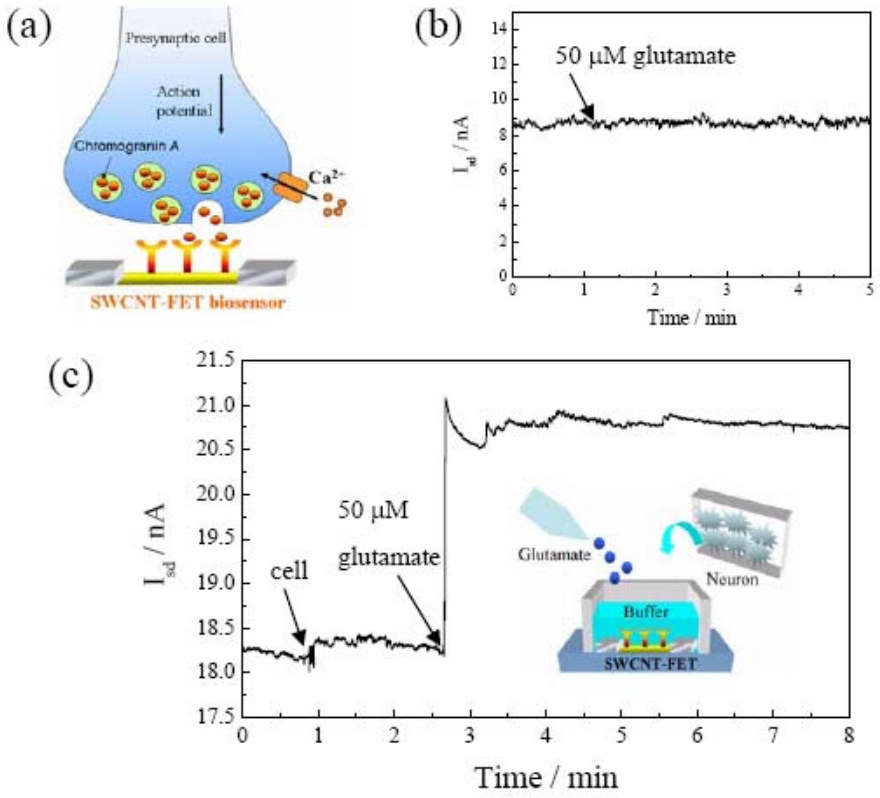

Figure 6. The CgA released from neurons can be detected by CgA-Ab/SWCNT-FETs. (a) When neurons are stimulated by glutamate, the voltage-gated Ca^{2+}channels at the axon terminal will be opened and allow the entrance of Ca^{2+} into the cytosol. The Ca^{2+} will induce the fusion of synaptic vesicles with plasma membrane to release CgA, which will then bind to the CgA-Ab immobilized on the SWCNT-FET. (b) Before the neuron experiment, a negative control without neurons on the FET device was performed by adding 50 μM glutamate to the CgA-Ab/SWCNT-FET. No I_{sd} change could be detected. (c) In-situ detection of the I_{sd} changes elicited by glutamate. The coverslip was positioned onto the FET device with neurons faced the circuit as illustrated by the inset cartoon and indicated by "cell" in the current trace. Glutamate (50 μM) was then added to stimulate the neurons to release CgA. The I_{sd} was measured in the ambient solution at V_{sd} = 10 mV with modulation frequency of 377.7 Hz throughout the experiment.

After the addition of 50 μM glutamate to activate the glutamate receptors, a huge increase in the I_{sd} of CgA-Ab/SWCNT-FET was detected as shown in Figure 6c.

CgA is widely detectable in central nervous system and is suggested to be co-released with the neurotransmitters.[16] Although CgA can also be a marker for neuron labeling, there are only very few reports measuring the release of CgA from neurons.[30] Some immunoassay kits for detecting CgA in serum have been developed and the detection limit is at ~nM level.[31] However, these techniques could not be used to monitor the low amount of CgA released from cultured neurons in real time. Moreover, after glutamate stimulation, the low amount of CgA released in the bath buffer could not be detected by Western blot either (data not shown). In contrast, our FET setup which directly measures the immediate vicinity release of CgA from neurons provides a novel technique to monitor the neuron activities.

It is noted that the little increase in I_{sd} when neurons were mounted onto the CgA-Ab/SWCNT-FET device (as marked by "cell" in Figure 6c) might be due to the basal release of CgA. This small current change, however, did not affect the instant and prominent I_{sd} increase when neurons were stimulated by glutamate. In the neuron experiment, we also tested the selectivity of bare SWCNT-FET devices (without the immobilization of CgA-Ab on the SWCNTs) by adding 50 μM glutamate to the neurons in 100 μL normal saline buffer. Again, no significant changes could be observed in this control experiment. These results suggest that the surface functionalized CgA-Ab/SWCNT-FETs are of detection specificity and can be applied to monitor the molecules released from living neurons.

3. Summary

Compared with the traditional time-consuming electrophoresis technique, e.g. Western blot, our study has demonstrated that the CgA released from the synaptic terminal of neurons can be detected in-situ by the CgA-Ab/SWCNT-FETs with high selectivity, sensitivity, and real-time detection capabilities. This sensory technique is promising in medical diagnosis and can further be applied to study the activity of individual neurons, which should open a new window to enlighten the neurophysiology in neuronal network.

4. Experimental section

4.1 Electrical measurement and optical imaging

In the electric transport measurements, the conductance of SWCNT-FET was recorded by a lock-in amplifier (Stanford Research 830) in an AC mode. To measure the I_{sd}-V_g curves, a power supply (Keithley 2400) was employed to apply the backgate voltage. The I_{sd}-V_g curves for CgA-Ab/SWCNT-FETs were measured after the CgA-Ab/SWCNT-FETs were fully rinsed with deionized water and dried in the ambient air. In this study, while the I_{sd}-V_g measurements (Figures 2 and 3) were performed in the ambient air, the I_{sd} vs. time experiments (Figures 4 and

6) were carried out in the ambient aqueous solutions. The fluorescence image after the immobilization of CgA-Ab onto SWCNTs (Figure 3c) was taken by an epifluoresce microscope (Nikon TE2000) with 20× objective, and the images of the CgA immnostaings (Figures 5a~d) were taken by a microscope (Leica DM-IRE) with 40× and 100× objectives.

4.2 Surface functionalization

In the processes of the surface functionalization of SWCNT-FETs, all sample solutions were driven by a syringe pump at the flowing rate of 0.5~0.8 mL/hr into the PDMS microfluidic channel coupled with the device arrays. The SWCNTs were first treated in 7.5 mM 1-pyrenebutanoic acid succinimidyl ester (Sigma Aldrich) for 1 hr and then flushed with pure methanol for 15 min. Subsequently, the device was incubated for 2 hr in PBS (pH 7.4) containing 0.2 μg/mL of goat IgG antibody against CgA. After the extra CgA-Ab was washed off, the device was then incubated for 20 min in PBS containing 0.5% tween 20 (J. T. Baker).

Reference

[1] Y. Cui, Q. Wei, H. Park, C. M. Lieber, *Science* **2001**, *293*, 1289.

[2] R. J. Chen, H. C. Choi,, S. Bangsaruntip, E. Yenilmez,, X. W. Tang, Q. Wang, Y. Chang, H. Dai, *J. Am. Chem. Soc*. **2004**, *126*, 1563.

[3] G. Grüner, *Anal. Bioanal. Chem*. **2006**, *384*, 322.

[4] H. M. So, K. Won, Y. H. Kim, B. K. Kim, B. H. Ryu, P. S. Na, H. Kim, J. O. Lee, *J. Am. Chem. Soc*. **2005**, *127*, 11906.

[5] H. R. Byon, H. C. Choi, *J. Am. Chem. Soc*. **2006**, *128*, 2188.

[6] A. Star, E. Tu, J. Niemann, J. C. P. Gabriel, C. S. Joiner, C. Valcke, *Proc. Natl. Acad. Sci. USA* **2006**, *103*, 921.

[7] C. Li, M. Curreli, H. Lin, B. Lei, F. N. Ishikawa, R. Datar, R. J. Cote, M. E. Thompson, C. Zhou, *J. Am. Chem. Soc*. **2005**, *127*, 12484

[8] J. Hahm, C. M. Lieber, *Nano Lett*. **2004**, *4*, 51.

[9] G. Zheng, F. Patolsky, Y. Cui, W. U. Wang, C. M. Lieber, *Nat. Biotechnol*. **2005**, *23*, 1294.

[10] F. Patolsky, G. Zheng, O. Hayden, M. Lakadamyali, X. Zhuang, C.M. Lieber, *Proc. Natl. Acad. Sci. USA* **2004**, *101*,14017

[11] F. Patolsky, B. P. Timko, G. Yu, W. Fang, A. B. Greytsk, G. Zheng, C. M. Lieber, *Science* **2006**, *313*, 1100.

[12] M. H. Metz-Boutigue, Y. Goumon, J. M. Strub, K. Lugardon, D. Aunis, *Ann. NY Acad. Sci.* **2003,** *992*, 168.

[13] T. Lechner, C Adlassning, C. Humpel, W. A. Kaufmann, H. Maier, K. Reinstadler-Kramer, J. Hinterholzl, S. K. Mahata, K. A. Jellinger, J. Marksteiner, *Exp. Gerontol*. **2004**, *39*, 101

[14] S. H. Yoo, *J. Boil. Chem*, **1994**, *269*, 12001

[15] J. Ciesielski-Treska, G. Ulrich, L. Taupenot, S. Chasserot-Golaz, A. Corti, D. Aunis, M. F. Bader, *J. Biol. Chem*. **1998**, *273*, 14339.

[16] L. Taupenot, K. L. Harper, D. T. O'Connor, *N. Engl. J. Med*. **2003**, *348*, 1134.

[17] H. Hu, Y. Ni, V. Montana, R. C. Haddon, V. Parpura, *Nano. Lett.* **2004**, *4*, 507.

[18] M. F. Islam, E. Rojas, D. M. Bergey, A. T. Johnson, A. G. Yodh, *Nano Lett.* **2003**, *3*, 269.

[19] D. E. Johnston, M. F. Islam, A. G. Yodh, A. T. Johnson. *Nat. Mater*. **2005**, 4, 589

[20] F. Patolsky, G. Zheng, C. M. Lieber, *Nature Protocols* **2006**, *1*, 1711.

[21] R. J. Chen, Y. Zhang, D. Wang, H. Dai, *J. Am. Chem. Soc.* **2001**, *123*, 3838.

[22] R. J. Chen, S. Bangsaruntip, K. A. Drouvalakis, N. W. S. Kam, M. Shim, Y. Li, W. Kim, P. J. Utz, H. Dai, *Proc. Natl. Acad. Sci. USA* **2003**, *100*, 4984.

[23] S. Heinze, J. Tersoff, R. Martel, V. Derycke, J. Appenzeller, Ph. Avouris. *Phys. Rev. Lett.* **2002**, *89*, 106801.

[24] R. Martel, V. Derycke, C. Lavoie, J. Appenzeller, K. K. Chan, J. Tersoff, Ph. Avouris, *Phys. Rev. Lett.* **2001**, *87*, 256805.

[25] W. Kim, A. Javey, O. Vermesh, Q. Wang, Y. Li, H. Dai, *Nano Lett.* **2003**, *3*, 193.

[26] J. C. McDonald, D. C. Duffy, J. R. Anderson, D. T. Chiu, H. Wu, O. J. A. Schueller, G. M. Whitesides. *Electrophoresis*. **2000**, 21, 27.

[27] G. P. Bernini, A. Moretti, M. Ferdeghini, S. Ricci, C. Letizia, E. D, Erasmo, G. F. A. Salvetti, *Br. J. Cancer* **2001**, *84*, 636.

[28] G. T. Brewer, *J. Nerosci. Res*. **1995**, *42*, 674.

[29] C. Y. Pan, A. Jeromin, K. Lundstrom, S. H. Yoo, J. Roder, A. P. Fox, *J. Neurosci.* **2002,** 22, 2427.

[30] A. D. Smith, *Philos. T. Roy. Soc. B* **1971**, 261, 363.

[31] A. Zitella, A. Berruti, P. Destefanis, G. Mengozzi, M. Torta, C. Ceruti, G. Casetta, A. Mosca, A. Greco, L. Rolle, G. Aimo, E. Aroasio, A. Tizzani, L. Dogliotti, D. Fontana. *Clinica Chimica Acta*. **2007**, 377 103.

 doi:10.1111/j.1471-4159.2007.04584.x

Lysophospholipids regulate excitability and exocytosis in cultured bovine chromaffin cells

Chien-Yuan Pan,*,†,[1] Adonis Z. Wu*,[1] and Yit-Tsong Chen‡

*Institute of Zoology, National Taiwan University, Taipei, Taiwan
†Department of Life Science, National Taiwan University, Taipei, Taiwan
‡Department of Chemistry, National Taiwan University, Taipei, Taiwan

Abstract

Bioactive lysophospholipids (LPLs) are released by blood cells and can modulate many cellular activities such as angiogenesis and cell survival. In this study, the effects of sphingosine-1-phosphate (S1P) and lysophosphatidic acid (LPA) on excitability and exocytosis in bovine chromaffin cells were investigated using the whole-cell configuration of the patch-clamp. Voltage-gated Ca^{2+} current was inhibited by S1P and LPA pre-treatment in a concentration-dependent manner with IC_{50}s of 0.46 and 0.79 μmol/L, respectively. Inhibition was mostly reversible upon washout and prevented by suramin, an inhibitor of G-protein signaling. Na^+ current was inhibited by S1P, but not by LPA. However, recovery of Na^+ channels from inactivation was slowed by both LPLs. The outward K^+ current was also significantly reduced by both LPLs. Chromaffin cells fired repetitive action potentials in response to minimal injections of depolarizing current. Repetitive activity was dramatically reduced by LPLs. Consistent with the reduction in Ca^{2+} current, exocytosis elicited by a train of depolarizations and the ensuing endocytosis were both inhibited by LPL pre-treatments. These data demonstrate the interaction between immune and endocrine systems mediated by the inhibitory effects of LPLs on the excitability of adrenal chromaffin cells.

Keywords: action potential, chromaffin cell, endocytosis, exocytosis, ion channels, lysophospholipids.
J. Neurochem. (2007) 10.1111/j.1471-4159.2007.04584.x

Sphingosine-1-phosphate (S1P) and lysophosphatidic acid (LPA) are two lysophospholipids (LPLs) secreted by platelets and macrophages during blood clotting and inflammation, respectively (Xiao *et al.* 2000; Okajima 2001). They have been reported to be involved in Ca^{2+} mobilization, cell survival and wound healing (Panetti 2002; Xu *et al.* 2003). These LPL-related responses are mainly mediated by cell surface G-protein coupled receptors (GPCRs) (Taha *et al.* 2004; Rosen and Goetzl 2005). At least five receptor subtypes have been linked to S1P signaling and three have been linked to signaling by LPA (Anliker and Chun 2004).

Several lines of evidence have demonstrated that S1P and LPA regulate the activities of ion channels. Most of these studies focused on endothelial, neuronal or fibroblast cells. S1P has been found to activate non-selective cation channels and large-conductance Ca^{2+}-activated K^+ channels (BK) in human endothelial cells (Muraki and Imaizumi 2001; Kim *et al.* 2006). It has also been reported that S1P inhibits voltage-gated K^+ current (I_K) in rat cerebral artery (Coussin *et al.* 2003) and LPA activates BK current in microglial cells (Schilling *et al.* 2004). Both S1P and LPA have been found to activate Cl^- current in cultured corneal keratinocytes (Wang *et al.* 2002) and myofibroblasts (Yin and Watsky 2005). In dorsal root ganglion neurons, LPA inhibits tetrodotoxin (TTX)-sensitive sodium current (I_{Na}) but enhances TTX-insensitive I_{Na} (Seung Lee *et al.* 2005). The exposure of rat

Received August 10, 2006; revised manuscript received February 21, 2007; accepted February 26, 2007.

Address correspondence and reprint requests to Dr C.-Y. Pan, Institute of Zoology, National Taiwan University, Rm730, Life Science Building, 1 Roosevelt Rd., Sec. 4, Taipei 106, Taiwan. E-mail: cypan@ntu.edu.tw or Dr Y.-T. Chen, Department of Chemistry, National Taiwan University, and Institute of Atomic and Molecular Sciences, Academia Sinica, PO Box 23-166, Taipei 106, Taiwan. E-mail: ytcchem@ntu.edu.tw

[1]C.-Y. Pan and A. Z. Wu contributed equally to this study.

Abbreviations used: AHP, afterhyperpolarization potential; AP, action potential; BK, large-conductance Ca^{2+}-activated K^+ channels; GPCR, G protein coupled receptor; HBSS, Hank's balanced salt solution; I_{Ca}, Ca^{2+} current; I_K, K^+ current; I_{Na}, Na^+ current; LPA, lysophosphatidic acid; LPL, lysophospholipid; NMG, *N*-Methyl-D-glucamine; PLC, phospholipase C; PTX, Pertussis toxin; S1P, sphingosine-1-phosphate.

sensory neurons to S1P enhances the frequency of action potential (AP) firing (Zhang *et al.* 2006). However, there is little information concerning the regulatory roles of LPLs in neurotransmitter release and AP firing.

A variety of voltage-gated ion channels can be identified on the plasma membrane of adrenal chromaffin cells, which secrete catecholamines in response to splanchnic nerve stimulation under physiological conditions. Calcium influx through calcium channels is the main factor responsible for catecholamine release from chromaffin cells (Douglas and Rubin 1961; Douglas and Poisner 1962; Boarder *et al.* 1987). In addition, APs can be evoked in cultured chromaffin cells (Kidokoro and Ritchie 1980). Therefore, it is an excellent model for studying electrical excitability and associated exocytosis (Winkler 1993). In addition, modulation of stimulus-secretion coupling in chromaffin cells by LPLs may play an important role in the interaction between immune and endocrine systems.

This study was designed to determine: (a) whether S1P and LPA affect calcium currents (I_{Ca}), I_K, and I_{Na} in cultured bovine adrenal chromaffin cells; (b) the effects of LPLs on AP firing and (c) how LPLs modulate stimulus-secretion coupling. Our results suggest that LPLs attenuate the activities of voltage-gated cationic channels, reduce AP firing and play an important role in modulating the release of catecholamines from chromaffin cells.

Materials and methods

Chemicals

Oleoyl-L-α-lysophosphatidic acid (LPA, C18:1, 1-oleoyl-*sn*-glycerol-3- phosphate), D-erythro-sphingosine-1-phosphate (S1P) and suramin sodium salt were purchased from Sigma (St. Louise, MO, USA). Pertussis toxin (PTX) and U73122 were obtained from CalBiochem (EMD Biosciences, San Diego, CA, USA). Dulbecco's modified Eagle's medium, fetal bovine serum, and Hank's balanced salt solution (HBSS) were purchased from Invitrogen Corp (Carlsbad, CA, USA). All other chemicals were commercially available and of reagent grade from Sigma. S1P and LPA were dissolved in chloroform : methanol/1:19 solution to a concentration of 1 mmol/L. It was then air-dried and redissolved in ethanol to make a stock of 1 mmol/L and stored at −20°C.

Solutions

The composition of normal HBSS bath solution for recording was as follows (in mmol/L): 138 NaCl, 5.3 KCl, 1.8 $CaCl_2$, 0.5 $MgCl_2$, 0.4 $MgSO_4$, 4 $NaHCO_3$, 0.34 Na_2HPO_4, 0.44 KH_2PO_4, 10 Hepes, 5.6 glucose, pH 7.3. In some experiments, the concentration of $CaCl_2$ was changed as indicated. To isolate I_{Na}, Ca^{2+}-free HBSS solution was used; to isolate I_{Ca}, cells were incubated in *N*-methyl-D-glucamine (NMG) solution (in mmol/L): 130 NMG, 2 KCl, 5 $CaCl_2$, 1 $MgCl_2$, 5.6 glucose, 10 Hepes, pH 7.3. For measuring I_{Na} or I_{Ca}, the patch pipette was filled with a Cs^+-containing solution (in mmol/L): 130 Cs-aspartate, 20 KCl, 1 $MgCl_2$, 0.1 EGTA, 3 Na_2ATP, 0.1 Na_2GTP and 20 Hepes, pH 7.3. To record membrane potential or I_K, cells were incubated in HBSS and the patch pipette was filled with a K^+-containing solution (in mmol/L): 130 K-aspartate, 20 KCl, 1 $MgCl_2$, 0.1 EGTA, 3 Na_2ATP, 0.1 Na_2GTP and 20 Hepes, pH 7.3.

To characterize the long-term effects of LPLs on inward currents, cells were incubated in HBSS containing LPL of different concentrations for 1 h before the start of recording. To identify the involvement of G-protein signaling pathway, cells were pre-treated with PTX (0.1 μg/mL) overnight; suramin (0.1 mmol/L) or U73122 (0.1 mmol/L) for 1 h. These chemicals were present before the establishment of the whole-cell configuration of patch-clamp technique and remained in the bath buffer during recording. For short-term treatment, S1P and LPA were added into the bath after a cell has already been whole-cell patched.

Cell preparation

Chromaffin cells were prepared by digestion of bovine adrenal gland obtained from local slaughterhouses with collagenase (0.5 mg/mL) and purified by density gradient centrifugation at 200 *g* as previously described (Pan *et al.* 2002). In brief, cells were plated at a density of 2×10^5 cells per 35-mm culture dish on poly L-lysine-coated coverslips and cultured in Dulbecco's modified Eagle's medium supplemented with 10% of fetal bovine serum. The medium was replaced every two days. All experiments were carried out between 5 and 10 days after cells were isolated.

Electrophysiological measurements

Cells were transferred to a recording chamber mounted on the stage of an inverted microscope and bathed in HBSS at 25°C. Patch pipettes were pulled from thin-wall capillaries with filament (Catalog 617000, A-M Systems Inc., Everett, WA, USA) using a two-stage microelectrode puller (P-97, Sutter Inc., Novato, CA, USA), and fire-polished with a microforge (MF-830, Narishige, Japan). When filled with pipette solution, the resistance ranged between 3–5 MΩ. To monitor the change in membrane capacitance, electrodes were coated with Sylgard (Catalog 184 Silicone Elastomer Kit, Dow Corning Co., Midland, MI, USA) to reduce nonspecific noise. Ionic currents, membrane capacitance, and APs were measured from whole-cell patch-clamped cells using an EPC10 patch-clamp amplifier (HEKA GmbH, Lambrecht, Germany) and controlled by Pulse software (HEKA GmbH).

For capacitance measurements, cells were whole-cell voltage clamped at −70 mV and depolarized with a train of 10 depolarizations to + 10 mV for 150 ms with an interval of 200 ms between the start of two consecutive depolarizations. A 10-ms sinewave with a frequency of 1 kHz and amplitude of 20 mV was applied just before the start of each depolarization to monitor the membrane capacitance. After the end of this train of depolarizations, the same sinewave was applied continuously and the capacitance measured was averaged every 100 ms. The membrane capacitance was obtained by the Lock-in amplifier using sine + dc mode in the Pulse software program.

To monitor the whole-cell inward I_{Na} and I_{Ca}, cells were voltage-clamped at a holding potential of −70 mV and depolarized to various potentials for 30 ms once every 15 s. The maximal inward current obtained during the first 5 ms was identified as I_{Na} and the current recorded between 18 and 27 ms of depolarization as I_{Ca}. For outward I_K, cell was depolarized to various potentials for 0.4 s the current during the last 100 ms of depolarization was averaged. To evoke

APs, cells were current clamped and adequate current was injected to bring the membrane potential slightly above threshold for 1.6 s.

To wash LPL out of the bath buffer, cell was placed in a perfusion chamber (JG-23 N/LP, Warner Instrument, US) containing 250 μL of NMG solution and patched with Cs^+-containing pipette solution to isolate the I_{Ca}. The cell was depolarized with 30 ms pulses to + 10 mV applied every 20 s from a holding potential of −70 mV. S1P or LPA was added directly to the bath to achieve a final concentration of 1 μmol/L. Five minutes later, the chamber was perfused continuously with NMG buffer containing no LPLs at a speed of 1 mL/min.

Data analysis

Signals were low-pass filtered at 3 kHz and stored in a Pentium III-based computer. Data are presented as mean ± SEM. For long-term LPL treatment, one-way analysis of variance with a least-significance difference method for multiple comparisons and unpaired Student's *t* test were used for statistical evaluation of differences among means. For short-term treatment, paired Student's *t* test was used to compare the results before and after the LPL addition. A value of $p < 0.05$ was considered to be statistically significant. The distributions of data were homogeneous as examined by Shapiro-Wilk Normality Test at 0.05 level.

The concentration-dependent inhibitory effects of LPLs on I_{Ca} and I_{Na} were fitted to a Hill function where percent of remaining current $= 1 - (E_{max} \times [C]^n)/(IC_{50}^n + [C]^n)$, [C] represents the concentration of LPL; IC_{50} and n are the concentration of LPL required for 50% inhibition and the Hill coefficient, respectively; E_{max} is the LPL-induced maximal percent inhibition of I_{Ca}, with a non-linear least-squares fitting algorithm.

Normalized inactivation curves were fit to a Boltzmann function, using the least-squares method according to $I = 1/(1 + \exp[V - a/b])$, where V is the conditioning potential in mV, a is the membrane potential for half-maximal inactivation, and b is the slope factor of the inactivation curve.

Results

S1P inhibits both I_{Na} and I_{Ca}

To examine long-term effects of LPLs on inward currents, cells were incubated in HBSS containing different concentrations of S1P for 1 h before starting patch-clamp recording. Using this protocol, peak inward current (due largely to I_{Na}) and sustained inward current (due largely to I_{Ca}) from representative cells were both inhibited by S1P after 1 h pre-treatment (Fig. 1a). Concentration-response curves (Fig. 1b) obtained using depolarizations from a holding potential of −70 mV to + 10 mV gave concentrations for half-maximal inhibition (IC_{50}) of I_{Na} and I_{Ca} *of* 0.57 and 0.46 μmol/L, respectively. However, even at 0.01 μmol/L, about 20% of the I_{Na} was inhibited ($p < 0.05$). Application of 1 μmol/L S1P reduced mean I_{Na} from −1343.8 ± 204.7 to −684.1 ± 87.5 (Fig. 1c; $n = 11$ each; $p < 0.05$) and mean I_{Ca} from −265.4 ± 33.2 to −75.8 ± 13.5 pA (Fig. 1d; $p < 0.05$). Thus, long-term treatment with physiological concentrations of S1P in bovine chromaffin cells strongly reduces both I_{Na} and I_{Ca}.

LPA inhibits I_{Ca} but not I_{Na}

Unlike S1P, short-term LPA treatment inhibits I_{Ca} but not I_{Na} in chromaffin cells (Pan *et al.* 2006). A similar result was obtained for long-term treatment with LPA (Figs 2a–d). When depolarized to + 10 mV, the IC_{50} for the inhibitory effects of LPA on I_{Ca} was 0.79 μmol/L (Fig. 2b). At +10 mV, I_{Ca} was significantly decreased from −278.5 ± 44.7 to −149.8 ± 20.9 pA ($n = 11$ each, $p < 0.05$) by pre-treatment with 2.5 μmol/L LPA. Inhibition of mean I_{Na} was not insignificant (−1.34 ± 0.20 to −1.14 ± 0.16 nA). These results indicate that long-term treatment with LPA produces a concentration-dependent inhibition of I_{Ca}, but not I_{Na}, in bovine chromaffin cells.

S1P, not LPA, negatively shifts the steady-state inactivation of I_{Na}

Changes in the steady-state inactivation of I_{Na} affect cell excitability (Fernandez *et al.* 2005). To isolate effects of LPLs on cell excitability that are I_{Na}-dependent, cells were bathed in Ca^{2+}-free HBSS solution to avoid the influence of I_{Ca} and inactivation was studied using paired depolarizations. The first depolarization was a 100 ms conditioning pre-pulse to various potentials from the holding potential of −70 mV and was followed immediately by a second 20 ms test depolarization to + 10 mV. As the pre-pulse became more positive, I_{Na} in response to the second depolarization became smaller (Fig. 3a). Normalized steady state inactivation curves obtained by plotting I_{Na} of the second depolarization versus pre-pulse potential were fit with a Boltzmann function as described in the Materials and methods (Figs 3b and c). For control cells ($n = 7$), the pre-pulse potential for half inactivation (a) was −34.5 ± 0.3 mV and with slope factor (b) of 7.4 ± 0.26 mV; in presence of S1P, a is negatively shifted to −41.9 ± 0.53 mV ($n = 7$, $p < 0.01$) but b was not significantly changed (7.8 ± 0.4 mV). This contrasts with LPA pre-treatment which produced no significant effects on steady-state inactivation (Control ($n = 8$): $a = -34.6 \pm 0.4$, $b = 8.8 \pm 0.38$ mV; 2.5 μmol/L LPA ($n = 8$): $a = -38.1 \pm 0.36$ mV; $b = 8.6 \pm 0.32$ mV). Thus, S1P, but not LPA, shifts the voltage-dependence of Na^+ channels to more negative potentials.

Both S1P and lysophosphatidic acid prolong recovery of I_{Na} from inactivation

The rate at which Na^+ channels recover from inactivation determines the maximum frequency of AP firing (Lou *et al.* 2003). Recovery rate was measured using two depolarizations to + 10 mV separated by different time intervals (Fig. 4a). I_{Na} of the second pulse was normalized to that of the first pulse and plotted against the recovery interval (Figs 4b and c). For control cells, I_{Na} recovered almost completely after about 30 ms (Figs 4a–c). Pre-treatment with 1 μmol/L S1P prolonged recovery (Fig. 4b), as did pre-treatment with 2.5 μmol/L LPA (Fig. 4c). Fits of recovery

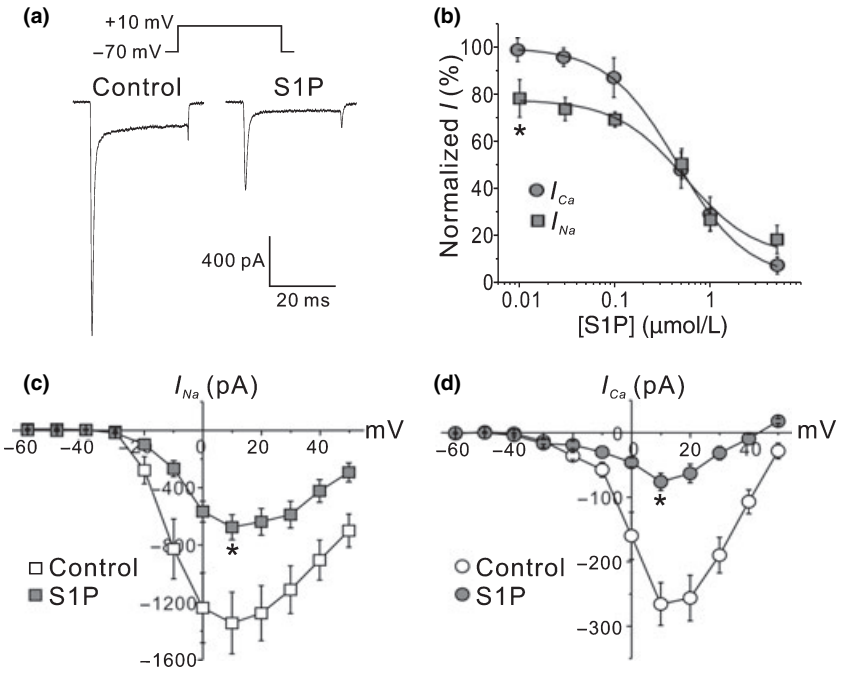

Fig. 1 Inhibitory effects of S1P on inward currents. Cells were bathed in Hank's balanced salt solution containing different concentrations of S1P for 1 h before and during whole-cell voltage-clamp recording using a Cs^+-containing pipette solution. Depolarizations (30 ms) to various potentials were applied once every 15 s from a holding potential of −70 mV. The inward maximal peak current was recorded as the Na^+ current (I_{Na}); the current between the 18th and 27th ms of the depolarization was averaged and recorded as the Ca^{2+} current (I_{Ca}). The concentration of $CaCl_2$ in the bath solution was 6.8 mmol/L. (a) Representative current traces during depolarizations to + 10 mV from untreated cells (Control) or treated with S1P (1 μmol/L) (S1P). (b) Concentration-dependent inhibitory effects of S1P on I_{Na} and I_{Ca}. The I_{Na} (■) and I_{Ca} (●) were acquired by a step-depolarization from a holding of −70 mV to + 10 mV for 30 ms under different concentrations of S1P. The currents were normalized to the averages obtained from control cells without S1P treatment. The concentration response was fit as described in Materials and methods. Sample number was at least 10 for each concentration. (c and d) Average *I–V* relations of I_{Na} and I_{Ca}, respectively, acquired in the absence (empty symbols) and presence (gray symbols) of 1 μmol/L S1P. Data are mean ± SEM from 11 cells each. *Student's *t*-test $p < 0.05$ when comparing to cells without S1P treatment.

times with a single-exponential function showed that S1P pre-treatment increased the time constant of the exponential from 8.1 ± 0.2 to 14.9 ± 0.6 ms ($n = 6$, $p < 0.001$) and LPA pre-treatment increased it from 7.8 ± 0.1 to 12.1 ± 0.3 ms ($n = 6$, $p < 0.01$). These results indicate that both LPA and S1P slow the recovery of I_{Na} from inactivation.

Pre-pulse cannot rescue the inhibited Ca^{2+} current

Application of strong depolarizing pre-pulses often reverses inhibition of I_{Ca} that is due to G-protein βγ subunits (Li *et al.* 2004). To determine whether I_{Ca} inhibited by LPLs could be rescued by such a protocol, cells were incubated in NMG buffer to isolate I_{Ca}. In control cells, a strong pre-pulse increased I_{Ca} recorded during a test pulse to + 10 mV. When the same protocol was repeated 2 min after addition of S1P, I_{Ca} was inhibited as described in Fig. 1 and no facilitation was observed (Fig. 5a). The mean results show that the I_{Ca} was facilitated by a strong pre-pulse from −226.3 ± 22.3 to −266.3 ± 29.5 pA in control ($n = 8$, $p < 0.05$), but not after addition of S1P, where an insignificant decrease from −161.5 ± 15.9 to −152.6 ± 15.5 pA was observed (Fig. 5b). Similarly, a conditioning pre-pulse increased I_{Ca} from −209.8 ± 21.9 to −258.2 ± 26.6 pA ($n = 8$, $p < 0.05$) before LPA treatment, but not after LPA treatment (from −161.7 ± 12.4 to −166.2 ± 13.7 pA) (Fig. 5c). These results indicate that the inhibitory effects of LPLs on I_{Ca} are not relieved by strong depolarizations, suggesting that inhibition is not mediated by the binding of $G_{\beta\gamma}$ subunits to Ca^{2+} channels in bovine chromaffin cells.

I_{Ca} recovers from inhibition after lysophospholipid washout

The concentration of LPLs in serum will eventually decrease to basal level after wounding. To ask whether the inhibition induced by both S1P and LPA is reversible, the LPLs in the recording chamber were washed out by continuous perfusion (Fig. 6). After beginning whole-cell recording in NMG buffer, I_{Ca} in cells was monitored every 20 s with a depolarization from a holding potential of −70 mV to + 10 mV. There was little rundown during the first 3 min of recording. S1P (1 μmol/L) or LPA (1 μmol/L) were then added directly to the chamber. The magnitude of I_{Ca} decreased slowly and

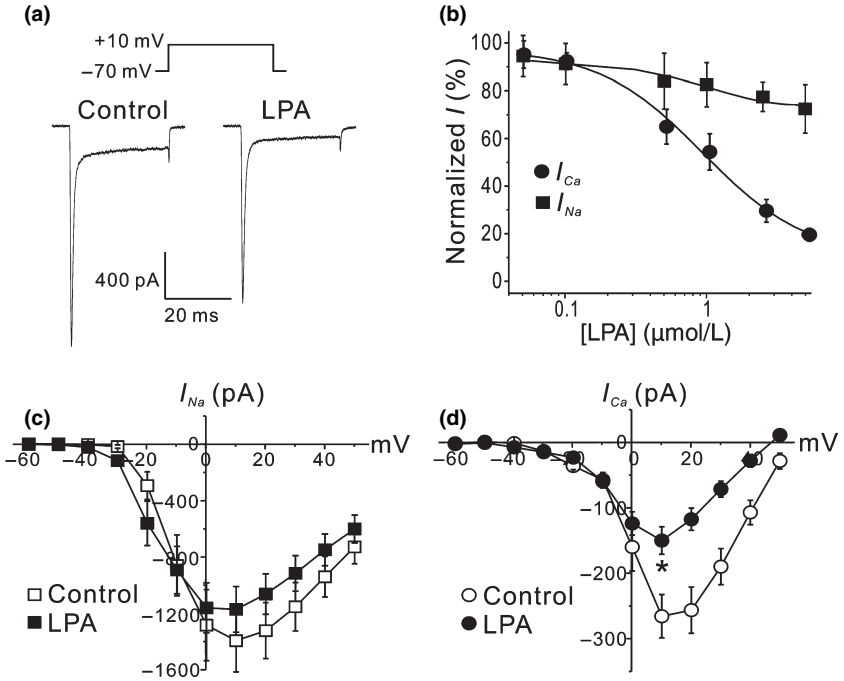

Fig. 2 Inhibitory effects of lysophosphatidic acid (LPA) on inward currents. Cells were bathed in Hank's balanced salt solution containing different concentrations of LPA for 1 h before and during whole-cell voltage-clamp recording using a Cs^+-containing pipette solution. Depolarizations (30 ms) to various potentials were applied once every 15 s from a holding potential of −70 mV. The inward maximal peak current was recorded as the Na^+ current (I_{Na}); the current between the 18th and 27th ms of the depolarization was averaged and recorded as the Ca^{2+} current (I_{Ca}). The concentration of $CaCl_2$ in the bath solution was 6.8 mmol/L. (a) Representative current traces from cells treated without (Control) or with 2.5 μmol/L LPA when depolarized to + 10 mV. (b) Concentration-dependent inhibitory effects of LPA on I_{Na} and I_{Ca}. Patched cells were depolarized to + 10 mV; I_{Na} (■) and I_{Ca} (●) acquired under different concentrations of LPA were normalized to the averages of cells not treated with LPA. The concentration response was fit as described in Methods. Sample number is at least 12 for each concentration. (c and d) Average *I–V* relations of I_{Na} and I_{Ca}, respectively, acquired in the absence (empty symbols) and presence (black symbols) of 2.5 μmol/L LPA. Data are mean ± SEM from 11 cells each. *Student's *t*-test $p < 0.05$ when compared to cells without LPA treatment.

continuously. Five min after addition of S1P or LPA, currents had decreased to 61.5 ± 0.4 and 72.8 ± 1.2%, respectively, of their initial levels. Washout of the compounds resulted in recovery to 88.5 ± 5.2 and 93.0 ± 2.9% of their initial levels, after 9 min for S1P and LPA, respectively. These results suggest that inhibition of I_{Ca} by short-term treatment with LPL is reversible.

Suramin antagonizes the inhibitory effects of S1P and lysophosphatidic acid

To define the involvement of GPCR pathways in the inhibitory effects of S1P and LPA on I_{Ca}, cells were pre-treated with U73122, an inhibitor of phospholipase C (PLC) (Noh *et al.* 1998), PTX, an inhibitor of $G_{i/o}$ (van Corven *et al.* 1989); or suramin, a general inhibitor of GPCR activation (Ancellin and Hla 1999) (Table 1). Though basal I_{Ca} was significantly inhibited by PTX and U73122 pre-treatments, application of S1P or LPA for 5 min further reduced the I_{Ca}. On the contrary, basal I_{Ca} was significantly and slightly elevated by suramin. In addition, in the presence of suramin, application of S1P or LPA only marginally inhibited I_{Ca}. These results suggest that LPL may inhibit the I_{Ca} through activation of GPCRs, but PLC and $G_{i/o}$ pathways may not be involved.

S1P and lysophosphatidic acid inhibit outward currents

Action potential repolarization is mostly due to activation of K^+ channels. To characterize the effects of LPLs on chromaffin cells, whole-cell outward I_K was monitored. After the incubation of chromaffin cells in S1P- or LPA-containing bath solution for one hour, I_K was inhibited when depolarized from a holding potential of −70 mV to various potentials (Fig. 7a). Averaged *I–V* relationships (Fig. 7b) show that I_K was inhibited at all potentials. At + 50 mV, the magnitude of I_K was significantly reduced by S1P and LPA to 52.1 ± 6.6 ($n = 6$, $p < 0.01$) and 44.5 ± 5.7% ($n = 6$, $p < 0.01$) of the current measured from cells without LPL treatment ($n = 8$), respectively (Fig. 7c). Inhibition of I_K was rapid, being decreased to 67.4 ± 12.1 or 57.6 ± 11.7% of the initial current by S1P (1 μmol/L) or LPA (2.5 μmol/L)

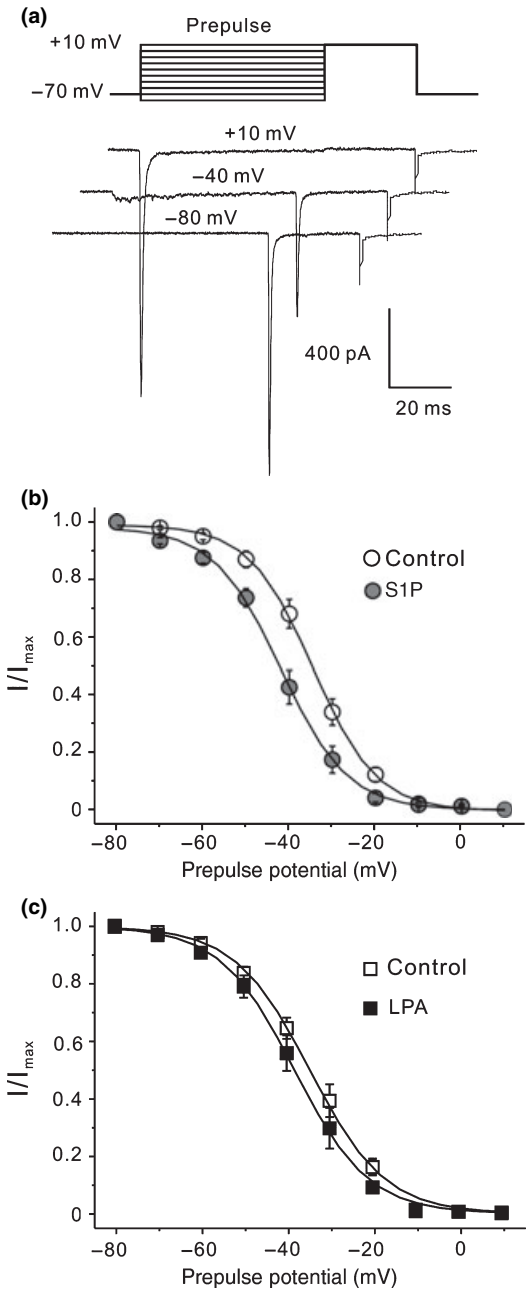

Fig. 3 Effects of lysophospholipids on the steady-state inactivation of I_{Na}. Cells were bathed in Ca^{2+}-free Hank's balanced salt solution and treated with S1P (1 μmol/L) or LPA (2.5 μmol/L) for 1 h before and during whole-cell voltage-clamp recording using a Cs^{+}-containing pipette solution. Cells were depolarized with a conditioning pulse to various potentials for 100 ms followed by a 20 ms depolarization to + 10 mV. The peak inward current during the second depolarization was measured as a function of conditioning pulse potential. (a) Representative traces from a control cell with conditioning pulses to −80, −40, and + 10 mV as indicated. (b and c) Normalized amplitude of I_{Na} (I/I_{Max}) plotted against the conditioning pre-pulse for cells treated with S1P and LPA, respectively. Data are mean ± SEM and fit to the Boltzmann equation as described in Materials and methods (n = 7–8 for each point).

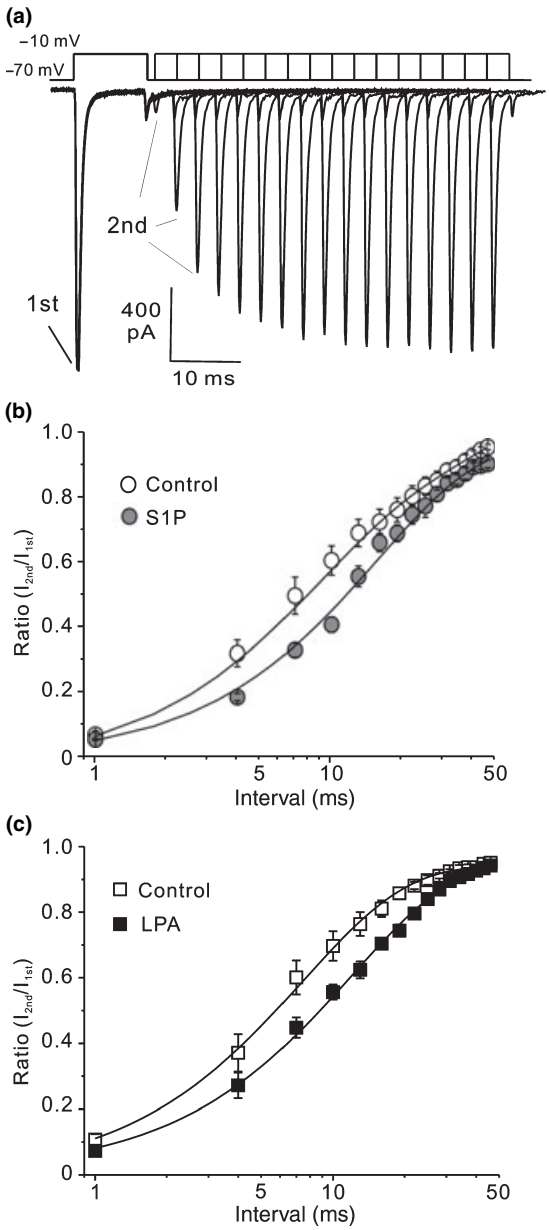

Fig. 4 Effects of lysophospholipids on the recovery rate of I_{Na}. Cells were bathed in Ca^{2+}-free Hank's balanced salt solution and pre-treated with S1P (1 μmol/L) or LPA (2.5 μmol/L) for 1 h before and during whole-cell voltage-clamp recording using a pipette filled with a Cs-containing solution. Cells were first depolarized to −10 mV for 10 ms from a holding potential of −70 mV. After a variable interval, a second pulse to −10 mV for 20 ms was applied. (a) Overlapping representative current traces from a control cell with different interpulse intervals from 1 to 46 ms. (b and c) I_{Na} ratio (I_{2nd}/I_{1st}) plotted against interpulse intervals for cells treated with S1P & LPA, respectively. Curves were fitted by a first-order exponential growth equation. Data are mean ± SEM (n = 6 for each treatment).

(n = 10, $p < 0.01$ for both), respectively, just 2 minutes after their application. These results indicate that voltage-gated I_K is also inhibited by LPL treatment.

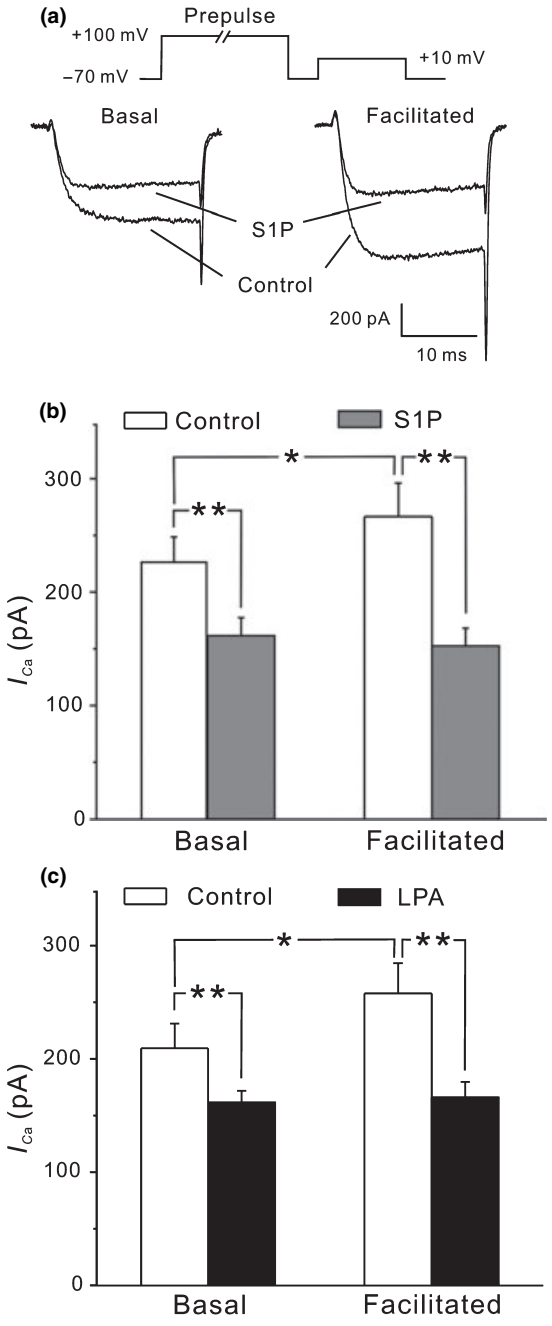

Fig. 5 Effect of LPLs on facilitated I_{Ca}. Cells were bathed in NMG solution containing 5 mmol/L $CaCl_2$ and whole-cell voltage -clamped with a Cs^+-containing pipette solution. Cells were depolarized to + 10 mV for 20 ms with or without a 100 ms conditioning pre-pulse to + 100 mV that preceded the test pulse by 5 ms. After recording a pair of basal (without pre-pulse) and facilitated (with pre-pulse) currents, S1P (1 μmol/L) or lysophosphatidic acid (LPA) (2.5 μmol/L) was added to the recording chamber. Two minutes later another pair of basal and facilitated currents was recorded. (a) Representative basal and facilitated current traces from a cell before (Control) and 2 min after (S1P) the addition of S1P. (b and c) Averaged baseline and facilitated I_{Ca} treated with S1P and LPA, respectively. Data are Mean ± SEM (n = 8 for each treatment). *Student's t-test $p < 0.05$; **$p < 0.01$.

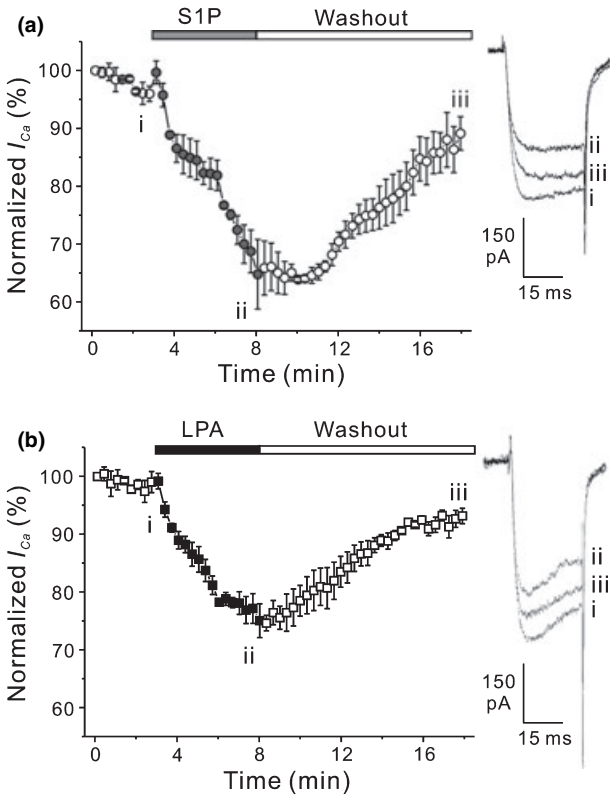

Fig. 6 Inhibition of I_{Ca} is reversible. Cell was bathed for 15 min in NMG buffer and voltage-clamped with Cs^+-containing buffer to isolate I_{Ca}. I_{Ca} was measured by a 30 ms step depolarization from −70 to + 10 mV applied once every 15 s. Three min after beginning whole-cell recording, 1 μmol/L of S1P (a) or lysophosphatidic acid (b) was added to the bath (gray or black bar above each graph). Five min later the recording chamber was continuously perfused with NMG buffer to wash out LPLs. The measured I_{Ca} was plotted against time. The current traces on the right were recordings before the addition of LPLs (i); before the perfusion (ii) and the last recording (iii) from a representative cell. Data presented are mean ± SEM; sample numbers are 3 for each group.

S1P and LPA decrease the firing frequency of action potentials

The above results showing that the both voltage-gated I_{Na} and I_K are inhibited by LPLs suggested that AP firing will also be modulated by LPLs. To verify this, cells were recorded in whole-cell configuration under current clamp mode and APs were evoked by minimal current injection. Representative results (Fig. 8a) showed that multiple AP could be elicited from cells in control, but only one AP could be elicited from cells pre-treated with LPLs for 1 h. An average of 4.4 ± 0.4 spikes/s (n = 8) could be elicited by a 1.6-s suprathreshold depolarizing current injection in cells without LPL treatment (Fig. 8b). However, after being incubated in buffer containing S1P (1 μmol/L, n = 6) or LPA (2.5 μmol/L, n = 6) for 1 h., only a single AP could be evoked, no matter how much current was injected. A similar reduction in the frequency of AP firing was also observed

Pre-treatment	−S1P	+S1P	−LPA	+LPA
Control	−226.3 ± 22.3	−161.5 ± 15.6**	−209.7 ± 21.8	−161.7 ± 10.3**
PTX	−174.9 ± 23.9*	−110.6 ± 19.8**	−179.9 ± 12.9*	−125.6 ± 19.2**
U73122	−103.1 ± 10.3*	−60.1 ± 7.5**	−109.5 ± 13.5*	−83.1 ± 10.7**
Suramin	−283.3 ± 20.9*	−251.3 ± 20.6	−265.0 ± 23.8*	−215.8 ± 25.8

Table 1 Effects of G protein coupled receptor signaling antagonists on Ca^{2+} currents

Unit, pA.

Cells were bathed in HBSS and whole-cell voltage-clamped. I_{Ca} was obtained by step depolarization form −70 to + 10 mV for 20 ms before (−) and 5 min after (+) the addition of LPLs.

*Student's *t*-test $p < 0.05$ when compared with the current without antagonist pre-treatment.

**Paired Student's *t*-test $p < 0.01$ when compared with the currents before the addition of S1P or LPA.

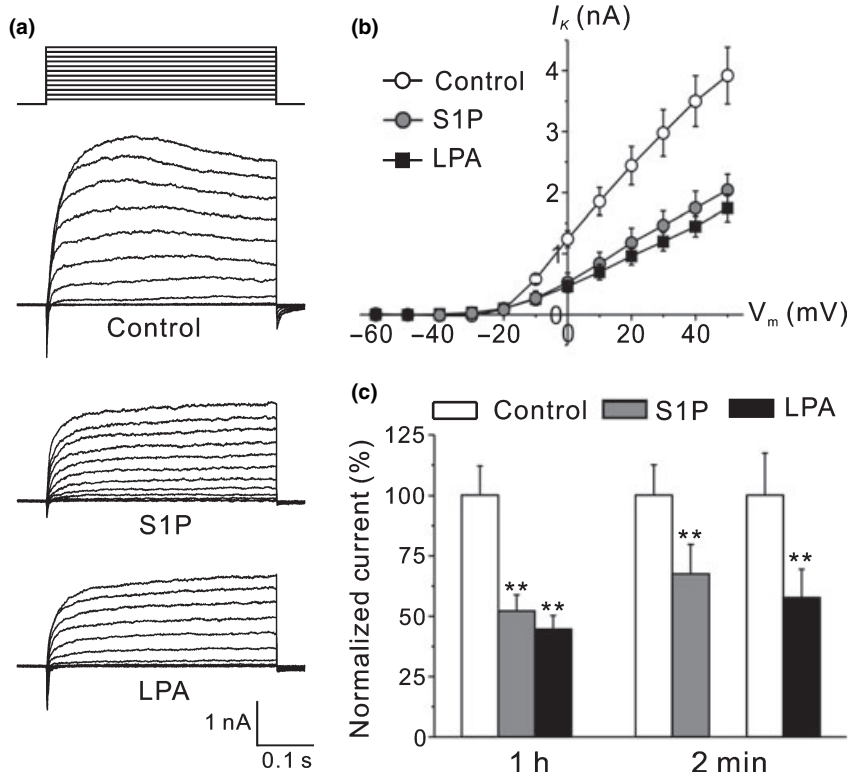

Fig. 7 Inhibitory effects of lysophospholipid (LPLs) on outward I_K. Cells were bathed in normal Hank's balanced salt solution and whole-cell voltage-clamped with a K^+-containing pipette solution. Cells were step depolarized to various potentials for 0.4 s and the outward current between 0.3 and 0.4 s during depolarization was averaged as I_K. For long-term treatment, cells were pre-treated with S1P (1 μmol/L, $n = 6$), LPA (2.5 μmol/L, $n = 6$) or without treatment (Control, $n = 8$) for 1 h before the establishment of whole-cell patch and same concentration of LPLs were used during the recording. For short-term treatment, S1P (1 μmol/L, $n = 10$) or LPA (2.5 μmol/L, $n = 10$) was added into the bath after the cell was whole-cell patched; the voltage-dependent I_K was recorded before (Control) and 2 min again after the addition of LPLs. (a) Representative I_K from cells pre-treated with LPLs as indicated for 1 h and step-depolarized to various potentials from a holding potential of −70 mV. (b) Averaged voltage-dependent I_K pre-treated with S1P (●) or LPA (■) for 1 h. (c) Normalized I_K acquired by step depolarization to + 50 mV from cells treated with LPL for long-term (1 h) or short term (2 min). Data are mean ± SEM. **Student's *t*-test $p < 0.01$ when comparing to control cells without (long-term) or before (short-term) LPL treatment.

2 minutes after the addition of LPL. The firing frequency was significantly reduced by S1P ($n = 7$) and LPA ($n = 6$) from 4.6 ± 0.4 and 4.2 ± 0.3 to 2.4 ± 0.3 and 2.7 ± 0.2 spikes/s, respectively, in 2 min.

The peak membrane potential reached by the first evoked AP (approximatedly + 44 mV) was not significantly changed by long- or short-term treatments with LPL. However, after being incubated in LPL-containing buffer for 1 h, the

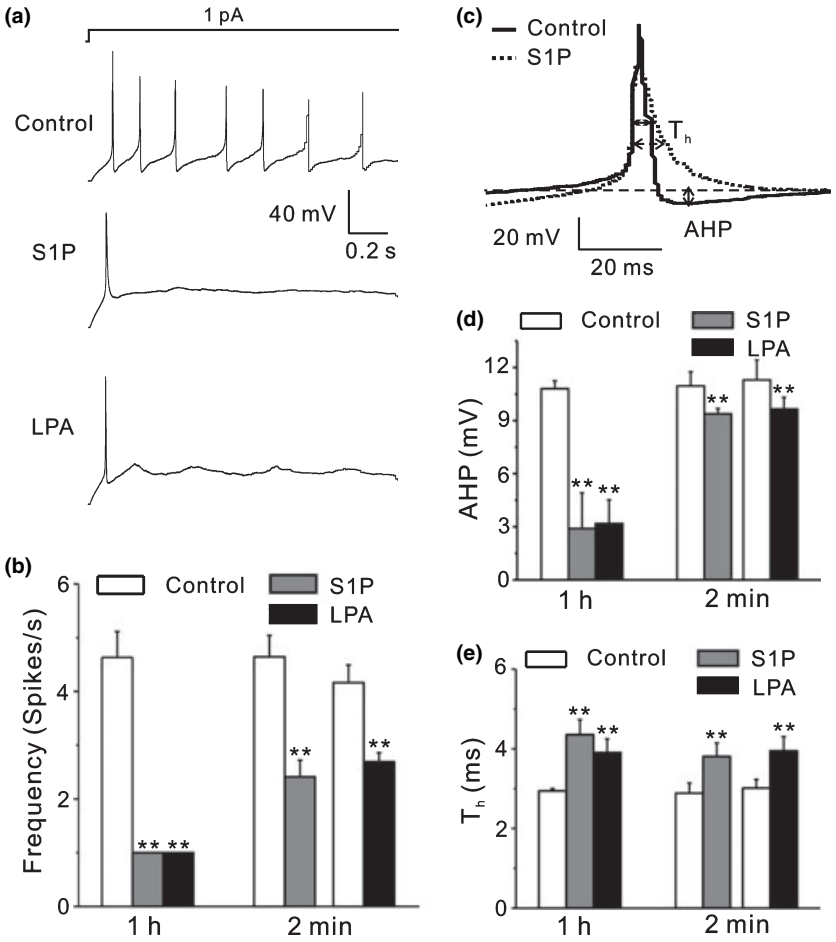

Fig. 8 Inhibitory effects of lysophospholipids (LPLs) on the firing frequency of action potentials (AP). Cells were bathed in normal hank's balanced salt solution and whole-cell recorded in the current-clamp mode with a K^+-containing pipette solution. For long-term treatment, cells were treated with S1P (1 μmol/L, $n = 6$), LPA (2.5 μmol/L, $n = 6$) for 1 h or without treatment (Control, $n = 8$) before the establishment of the whole-cell configuration and during recording. For short-term treatment, S1P (1 μmol/L, $n = 7$) or LPA (2.5 μmol/L, $n = 6$) was added into the bath after the cell was whole-cell clamped and the AP were evoked before (Control) and again 2 min after the application of LPLs. Cells were current clamped and injected with the minimal depolarizing current required to trigger AP for 1.6 s. (a) Representative membrane potential traces from long-term LPL-treated cells. Cells were current clamped and injected with 1 pA of current for 1.6 s as indicated. (b) Averaged frequency of AP (firing from cells long- (1 h) or short-term (2 min) treated with LPLs. (c) The first APs from a control (solid line) and a S1P (dotted line) long-term treated cells. The magnitude of the AHP, the difference between the lowest hyperpolarization potential and the normalized membrane potential (dashed line) during current injection; and half amplitude duration (T_h, double-arrow) were analyzed. (d) The averaged AHP from cells long- (1 h.) or short-term (2 min) LPL-treated cells. (e) The averaged T_h from long- (1 h.) and short-term(2 min) LPL-treated cells. Data are mean ± SEM. *Student's *t*-test $p < 0.05$ when comparing to that of control cells without (long-term) or before (short-term) LPL treatments.

difference (Fig. 8d) between the baseline potential during current injection and the maximal hyperpolarization potential following the AP (afterhyperpolarization potential, AHP) was strongly decreased from 10.7 ± 0.4 of control cells to 2.9 ± 2.0 and 3.2 ± 1.3 mV by long-term treatments with S1P and LPA, respectively. The AHP was slightly but significantly decreased by short-term treatment with S1P and LPA to 9.3 ± 0.3 and 9.6 ± 0.7 from 10.9 ± 0.8 and 11.2 ± 1.1 mV, respectively. The half-width duration (T_h) (Fig. 8e) of the first evoked AP was significantly increased from 3.0 ± 0.1 to 4.4 ± 0.4 and 3.9 ± 0.3 ms by long-term S1P and LPA treatment, respectively. Similarly, the T_h could also be significantly increased to 3.8 ± 0.3 and 4.0 ± 0.4 from 2.9 ± 0.3 and 3.0 ± 0.2 ms by short-term S1P and LPA treatment, respectively. These results illustrate that LPLs reduce repetitive AP firing, decrease AHPs and increase the width of APs in chromaffin cells.

S1P and LPA inhibit both exocytosis and endocytosis

To investigate whether the inhibition of I_{Ca} by LPLs leads to the modulation of exocytosis and endocytosis, the change in membrane capacitance evoked by a train of depolarizations

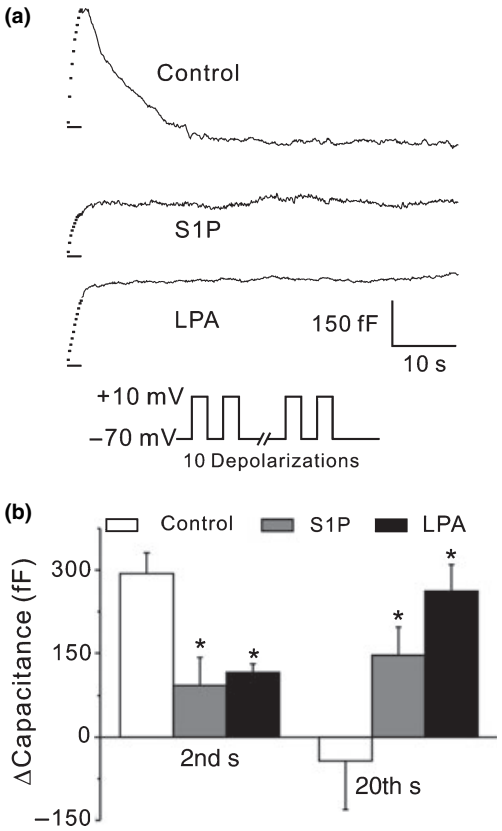

Fig. 9 Effects of lysophospholipids (LPLs) on depolarization-evoked exocytosis and endocytosis. Cells were bathed in normal HBSS containing 6.8 mmol/L $CaCl_2$ and pre-treated with S1P (1 μmol/L) or LPA (2.5 μmol/L) for 1 h. Same concentrations of LPLs were present in the recording bath. Cells were whole-cell patched with a Cs^+-containing pipette solution and stimulated with a train of 10 depolarizations to + 10 mV from a holding potential of −70 mV for 150 ms gapped with an interval of 50 ms. The membrane capacitance during and after the depolarizations was recorded. (a) Representative capacitance traces from cells not treated with LPL (Control), treated with S1P (S1P) or LPA (LPA). The black bar under each trace indicates the period of depolarizations. (b) Averaged changes in membrane capacitance at 2nd and 20th s after the start of the depolarization train. Data are mean ± SEM; sample numbers are 10, 12, and 15 for Control, S1P and LPA, respectively. *Student's *t*-test $p < 0.05$ when comparing to Control group.

was monitored (Fig. 9a). When exocytosis is evoked by membrane depolarization, the fusion of the secretory vesicles to the plasma membrane increases the surface area which is reflected in an increase in the membrane capacitance. On the contrary, the occurrence of endocytosis decreases the surface area and membrane capacitance. In a control cell, a train of 10 depolarizations resulted in a rapid increase in membrane capacitance. The increase declined to a level similar to that before stimulation in about 30 s (Fig. 9a). In cells pre-treated with LPLs for 1 h, the increase was small and did not decline after the stimulation. Average increases in capacitance during the train of depolarizations was 293.6 ± 37.6 fF for untreated cells (n = 10) but was significantly reduced to 93.2 ± 49.1 and 115.3 ± 15.5 fF after long-term treatment with S1P (1 μmol/L, n = 12) and LPA (2.5 μmol/L, n = 15), respectively (Fig. 9b). The capacitance measured 20s after stimulation relative to that before the train of depolarizations was −64.1 ± 75.2 fF for the control cell, and significantly increased to 146.4 ± 50.7 and 261.9 ± 48.1 fF for cells pre-treated with S1P and LPA, respectively. These results indicate that both exocytosis and endocytosis are suppressed by LPLs.

Discussion

Our study identified effects of LPLs on I_{Na}, I_{Ca}, and I_K, as well as on catecholamine secretion. We found that both S1P and LPA inhibit I_{Ca} in a concentration-dependent manner in isolated bovine chromaffin cells. These inhibitory effects of LPLs are mediated by GPCRs but $G_{\beta\gamma}$ may not be involved. In contrast to I_{Ca}, only S1P inhibits I_{Na}. However, both LPLs prolong the recovery rate of I_{Na}. Finally, both LPLs reduce I_K. We also showed that LPLs reduce repetitive firing of APs and inhibit both exocytosis and endocytosis. These results indicate that S1P and LPA at physiological concentrations attenuate the excitability of chromaffin cells and hint at the possible blockade of catecholamine secretion induced by sympathetic neurons.

The IC_{50} of S1P and LPA for inhibiting the inward currents are both well below 1 μmol/L. It has been reported that S1P concentrations in plasma and serum are about 0.2 and 0.5 μmol/L, respectively (Yatomi *et al.* 1997); the LPA concentration in serum is even higher, ranging between 1 and 10 μmol/L (Panetti *et al.* 2001). Our data show that approximately 20% of the I_{Na} is inhibited by S1P even at 0.01 μmol/L, implying that I_{Na} in chromaffin cells is partially modulated even in healthy people in the absence of stimulation. Further inhibition of Na^+ channels would occur when S1P is released from platelets during wounding or by macrophages during inflammation. On the contrary, basal levels of LPA (5 μmol/L) would have little effect on I_{Na}, but I_{Ca} would be inhibited by 80%.

Concentration-dependent inhibition of I_{Na} and I_{Ca} were both measured from the same traces but at different times during the trace. However, when I_{Na} was measured independently using Ca^{2+}-free HBSS buffer (Figs 3 and 4) or I_{Ca} was isolated using NMG buffer (Figs 5 and 6), the concentration-dependence of inhibition was approximately the same. The ability to approximate inhibition of I_{Na} and I_{Ca} separately from individual traces probably results from their different time courses. I_{Ca} activates slowly and reaches a maximum only after 5 ms (Fig. 5) whereas peak I_{Na} occurs in < 3 ms and then inactivates (Figs 3 and 4). The fact that LPA inhibited the I_{Ca}, but not I_{Na}, provides further evidence that I_{Na} is not contaminated by I_{Ca}.

Our results show that a strong depolarization pre-pulse cannot rescue the inhibition of I_{Ca} induced by LPLs.

Increased current following such a pre-pulse is a signature of inhibition that is due to binding of G protein βγ subunits to high voltage-activated calcium channels (Currie and Fox 2000; Li *et al.* 2004). Since we did not see an LPL-induced increase, it is unlikely that I_{Ca} inhibition was due to bound $G_{\beta\gamma}$ subunits that resulted from activation of GPCRs by LPLs. Consistent with this view, the facilitated currents observed following a strong pre-pulse in control cells are blocked by LPLs. The failure of the pre-pulse to facilitate current in LPL-treated cells may hint at a loss of intrinsic binding of $G_{\beta\gamma}$ subunits to Ca^{2+} channels (De Waard *et al.* 2005). However, how LPLs interfere with $G_{\beta\gamma}$ inhibition of Ca^{2+} channels requires further investigation.

U73122 completely prevents the elevation in $[Ca^{2+}]_i$ whereas PTX treatment inhibits only half of this elevation when stimulated by both LPLs (Pan *et al.* 2006). In addition to being an effective inhibitor of PLC, U73122 has multiple side effects by alkylation of various proteins (Horowitz *et al.* 2005) and block the voltage-gated Ca^{2+} channels on the differentiated NG108-15 cells (Jin *et al.* 1994). We found that U73122 by itself inhibits basal I_{Ca} (Table 1). It is unclear whether this is a specific effect due to inhibition of PLC, or a non-specific one, and was not investigated further. Whatever the non-specific effects, S1P or LPA inhibit the same fraction of I_{Ca}, whether or not cells have been pre-treated with U73122 or PTX. Therefore, it is unlikely that elevation in $[Ca^{2+}]_i$ is necessary for inhibition of I_{Ca} by LPLs.

We found that suramin largely blocked effects of LPLs on I_{Ca}, but also increased basal I_{Ca}. It has been reported that I_{Ca} can be inhibited by an autocrine mechanism through the activation of opioid and purinergic receptors mediated by $G_{\beta\gamma}$ subunits in chromaffin cells (Albillos *et al.* 1996; Carabelli *et al.* 2001). Suramin functions not only as a GPCR uncoupler (Chung and Kermode 2005) but also as a P_2 purinoreceptor blocker (Hoiting *et al.* 1990). This other effect of suramin may explain why suramin enhances the basal current in addition to antagonizing the inhibitory effect of LPLs. Therefore, our results with suramin indicate that activation of GPCRs is required for inhibition of I_{Ca} by LPLs. However, suramin may also affect other signaling pathways affecting I_{Ca}.

We show that I_K is reduced in the presence of LPLs. As measured here using conditions designed to minimally buffer intracellular Ca^{2+}, I_K in chromaffin cells consists of a voltage-dependent component as well as a Ca^{2+}-activated component that includes current through BK and small conductance Ca^{2+}-activated K^+ channels (SK) calcium channels (Marty 1981; Marty and Neher 1985; Artalejo *et al.* 1993). Inhibition of I_K by LPLs may be due to direct effects on any or all of the potassium channel types contributing to the total current. It is also possible that reduction in I_K may be secondary to reduced total amount of Ca^{2+} by inhibiting calcium entry via I_{Ca} as demonstrated here.

The original studies of chromaffin cell electrophysiology showed that the run-down in I_{Ca} leads to the decline of BK and that much of the outward I_K is carried by BK in cultured bovine chromaffin cells (Marty 1981; Marty and Neher 1985). In GH_3 pituitary cells, BK and Ca^{2+} currents have been suggested to be functionally coupled (Wu *et al.* 2001). Recently, Berkefeld *et al.* (2006) show that the antibody-purified BK channels from rat brain and chromaffin cells are assembled with voltage-gated L-, N-, and P/Q-type Ca^{2+} channels into a macromolecular complex; inhibiting the L- and P/Q-type Ca^{2+} currents also suppresses the BK currents in chromaffin cells (Berkefeld *et al.* 2006). The Ca^{2+} influx through the Ca^{2+} channels may therefore form a "Ca^{2+} microdomain" that activates the BK currents. The modulation of calcium channels by LPLs that we show is likely to modulate such a complex between BK channels and voltage-gated Ca^{2+} channels.

Ca^{2+}-activated I_K can also be activated by the release of Ca^{2+} from intracellular Ca^{2+} stores. Since LPLs release Ca^{2+} from intracellular stores (Pan *et al.* 2006), the resulting increase in intracellular calcium may activate BK and/or SK. In fact, histamine was shown to activate small conductance Ca^{2+}-activated K^+ channels (SK) in bovine chromaffin cells (Artalejo *et al.* 1993) and muscarinic stimulation activates BK and/or SK in guinea pig chromaffin cells (Ohta *et al.* 1998). These effects on Ca^{2+}-activated I_K may have been minimized in our study due to the use of the whole-cell patch configuration, the release of Ca^{2+} from intracellular Ca^{2+} stores by LPLs may not be able to activate most of the BK on the plasma membrane (Prakriya *et al.* 1996). Such increases in Ca^{2+}-activated I_K would counteract the reduction in I_K identified in the present study. Perforated whole-cell patch and $[Ca^{2+}]_i$ imaging studies in conjunction with specific toxins against BK and SK will be needed to clarify the roles that BK and SK play in the LPL-mediated modulation of stimulus-secretion coupling under physiological conditions.

Despite this caveat, our results are consistent with previous reports that the inhibition of BK will decrease the AHP, widen the spike, and attenuate repetitive AP firing in rat and bovine chromaffin cells (Lovell and McCobb 2001; Lovell *et al.* 2004). The delay in Na^+ channel recovery will further decrease the availability of Na^+ channels for repetitive AP firing. Therefore, after the first AP in LPL-treated cells, the membrane potential may not hyperpolarize strongly enough to allow inactivated Na^+ channels to recover from inactivation. These effects on Na^+ and K^+ channels will contribute to the suppression of AP firing that is observed after LPL treatment. Specific inhibitors against BK channels will be important for future study to verify how LPLs affect the I_K and AP firing in bovine chromaffin cells.

Propagation of APs in neurons is mainly determined by the cooperation of voltage-gated Na^+ and K^+ channels (Debanne 2004). Though our results show that the activities of these two channels in bovine chromaffin cells are both suppressed by LPLs; S1P has been reported to increase TTX-resistant I_{Na} and inhibits outward I_K in small diameter sensory neurons (Zhang *et al.* 2006). In these neurons, S1P results in sensitization by

increasing AP firing to transmit the inflammatory response. LPA has also been shown to enhance the AP firing of dorsal horn neurons by intraplantar injection to modulate the nociceptive processing (Elmes *et al.* 2004). These results contrast with ours and suggest that the excitability of different cells is differentially modulated by LPLs depending on their physiological activities. This differential modulation is likely to depend on different complements of ion channels and/or different regulatory cascades.

One of the most important characteristics of a chromaffin cell is to release catecholamines into the blood stream to modulate the fight-or-flight response. Ca^{2+} influx through the voltage-gated Ca^{2+} channels is the main pathway for triggering catecholamine secretion (Douglas and Rubin 1961; Douglas and Poisner 1962). Therefore, the decrease in exocytosis evoked by a train of depolarizations can be attributed to the inhibitory effects of LPLs on voltage-gated I_{Ca}. However, the total membrane capacitance does not decline to the level before the train of depolarizations suggesting that the endocytosis may be also blocked by LPLs. Endocytosis is also related to the changes in $[Ca^{2+}]_i$ (Schweizer and Ryan 2006) and the amount of membrane retrieval is normally proportional to the level of exocytosis to support future stimulation (Smith and Neher 1997; Engisch and Nowycky 1998). The decrease in Ca^{2+} influx by LPLs may affect both the machineries of exocytosis and endocytosis; however, it is also possible that LPLs modulate the cytoskeleton (Donati and Bruni 2006) or other proteins involved in exo-endocytosis to modulate stimulus-secretion coupling. Further experiments will be pursued to characterize how LPLs modulate the exo-endocytosis.

Macrophages synthesize over 100 distinct compounds including S1P and LPA (Nathan 1987). In rat and human adrenal glands, a population of macrophages distributed throughout the cortex and medulla (Schober *et al.* 1998) may provide a paracrine modulation pathway. Physiologically, the release of catecholamines from the adrenal glands is a signal to prepare the body for fight-or-flight response. The circulation system will be boosted to energize the muscle cells. However, when the body is hurt, the concentration of LPLs in blood will also be increased. At the beginning, more catecholamines will be released by the direct stimulatory effects of the LPLs on $[Ca^{2+}]_i$ in chromaffin cells as reported previously (Pan *et al.* 2006). Several minutes later, the Ca^{2+} channels are inhibited and the exocytosis will be suppressed as well. Meanwhile, acetylcholine released by the sympathetic neurons to stimulate the chromaffin cells will evoke less catecholamine secretion into the circulation system. When the concentrations of LPLs in serum return to normal levels, chromaffin cells will recover from the inhibition and their ability to secrete enough catecholamines to fully modulate physiological responses will return. Thus, the LPLs released by wounding or inflammatory response may modulate the physiological response to catecholamine secretion and ultimately, the status of the body, through their effects on the adrenal medulla.

Acknowledgements

The authors would like to gratefully thank Prof. Todd Scheuer (University of Washington) for help in writing the manuscript; Prof. Sheng-Nan Wu (National Cheng Kung University) for reading the manuscript and Prof. Hsin-Yu Lee (National Taiwan University) for help in LPL preparation. We also thank Mrs. Yong-Cyuan Chen, Po-Yuan Shih, and Ming-Ling Chen for help in the preparation of cultured cells and Tzu-Lun Wang for assistance with washout device setting. The work was supported by grants from the National Science Council (NSC 94-2311-B-002-008 and NSC 94-2627-M-002-003), Taiwan.

References

Albillos A., Gandia L., Michelena P., Gilabert J. A., del Valle M., Carbone E. and Garcia A. G. (1996) The mechanism of calcium channel facilitation in bovine chromaffin cells. *J. Physiol.* **494**, 687–695.

Ancellin N. and Hla T. (1999) Differential pharmacological properties and signal transduction of the sphingosine 1-phosphate receptors EDG-1, EDG-3, and EDG-5. *J. Biol. Chem.* **274**, 18997–19002.

Anliker B. and Chun J. (2004) Lysophospholipid G protein-coupled receptors. *J. Biol. Chem.* **279**, 20555–20558.

Artalejo A. R., Garcia A. G. and Neher E. (1993) Small-conductance Ca^{2+}-activated K^+ channels in bovine chromaffin cells. *Pflugers Arch.* **423**, 97–103.

Berkefeld H., Sailer C. A., Bildl W. *et al.* (2006) BK_{Ca}-Ca_v channel complexes mediate rapid and localized Ca^{2+}-activated K^+ signaling. *Science* **314**, 615–620.

Boarder M. R., Marriott D. and Adams M. (1987) Stimulus secretion coupling in cultured chromaffin cells. Dependency on external sodium and on dihydropyridine-sensitive calcium channels. *Biochem. Pharmacol.* **36**, 163–167.

Carabelli V., Hernandez-Guijo J. M., Baldelli P. and Carbone E. (2001) Direct autocrine inhibition and cAMP-dependent potentiation of single L-type Ca^{2+} channels in bovine chromaffin cells. *J. Physiol.* **532**, 73–90.

Chung W. C. and Kermode J. C. (2005) Suramin disrupts receptor-G protein coupling by blocking association of G protein alpha and betagamma subunits. *J. Pharmacol. Exp. Ther.* **313**, 191–198.

van Corven E. J., Groenink A., Jalink K., Eichholtz T. and Moolenaar W. H. (1989) Lysophosphatidate-induced cell proliferation: identification and dissection of signaling pathways mediated by G proteins. *Cell* **59**, 45–54.

Coussin F., Scott R. H. and Nixon G. F. (2003) Sphingosine 1-phosphate induces CREB activation in rat cerebral artery via a protein kinase C-mediated inhibition of voltage-gated K^+ channels. *Biochem. Pharmacol.* **66**, 1861–1870.

Currie K. P. and Fox A. P. (2000) Voltage-dependent, pertussis toxin insensitive inhibition of calcium currents by histamine in bovine adrenal chromaffin cells. *J. Neurophysiol.* **83**, 1435–1442.

De Waard M., Hering J., Weiss N. and Feltz A. (2005) How do G proteins directly control neuronal Ca^{2+} channel function? *Trends Pharmacol. Sci.* **26**, 427–436.

Debanne D. (2004) Information processing in the axon. *Nat. Rev. Neurosci.* **5**, 304–316.

Donati C. and Bruni P. (2006) Sphingosine 1-phosphate regulates cytoskeleton dynamics: Implications in its biological response. *Biochim. Biophys. Acta* **1758**, 2037–2048.

Douglas W. W. and Poisner A. M. (1962) On the mode of action of acetylcholine in evoking adrenal medullary secretion: increased uptake of calcium during the secretory response. *J. Physiol.* **162**, 385–392.

Douglas W. W. and Rubin R. P. (1961) The role of calcium in the secretory response of the adrenal medulla to acetylcholine. *J. Physiol.* **159**, 40–57.

Elmes S. J., Millns P. J., Smart D., Kendall D. A. and Chapman V. (2004) Evidence for biological effects of exogenous LPA on rat primary afferent and spinal cord neurons. *Brain Res.* **1022**, 205–213.

Engisch K. L. and Nowycky M. C. (1998) Compensatory and excess retrieval: two types of endocytosis following single step depolarizations in bovine adrenal chromaffin cells. *J. Physiol.* **506**, 591–608.

Fernandez F. R., Mehaffey W. H. and Turner R. W. (2005) Dendritic Na^+ current inactivation can increase cell excitability by delaying a somatic depolarizing afterpotential. *J. Neurophysiol.* **94**, 3836–3848.

Hoiting B., Molleman A., Nelemans A. and Den Hertog A. (1990) P2-purinoceptor-activated membrane currents and inositol tetrakisphosphate formation are blocked by suramin. *Eur. J. Pharmacol.* **181**, 127–131.

Horowitz L. F., Hirdes W., Suh B. C., Hilgemann D. W., Mackie K. and Hille B. (2005) Phospholipase C in living cells: activation, inhibition, Ca^{2+} requirement, and regulation of M current. *J. Gen. Physiol.* **126**, 243–262.

Jin W., Lo T. M., Loh H. H. and Thayer S. A. (1994) U73122 inhibits phospholipase C-dependent calcium mobilization in neuronal cells. *Brain Res.* **642**, 237–243.

Kidokoro Y. and Ritchie A. K. (1980) Chromaffin cell action potentials and their possible role in adrenaline secretion from rat adrenal medulla. *J. Physiol.* **307**, 199–216.

Kim M. Y., Liang G. H., Kim J. A., Kim Y. J., Oh S. and Suh S. H. (2006) Sphingosine-1-phosphate activates BK_{Ca} channels independently of G protein-coupled receptor in human endothelial cells. *Am. J. Physiol. Cell Physiol.* **290**, C1000–1008.

Li B., Zhong H., Scheuer T. and Catterall W. A. (2004) Functional role of a C-terminal Gbetagamma-binding domain of $Ca_v2.2$ channels. *Mol. Pharmacol.* **66**, 761–769.

Lou X. L., Yu X., Chen X. K., Duan K. L., He L. M., Qu A. L., Xu T. and Zhou Z. (2003) Na^+ channel inactivation: a comparative study between pancreatic islet beta-cells and adrenal chromaffin cells in rat. *J. Physiol.* **548**, 191–202.

Lovell P. V. and McCobb D. P. (2001) Pituitary control of BK potassium channel function and intrinsic firing properties of adrenal chromaffin cells. *J. Neurosci.* **21**, 3429–3442.

Lovell P. V., King J. T. and McCobb D. P. (2004) Acute modulation of adrenal chromaffin cell BK channel gating and cell excitability by glucocorticoids. *J. Neurophysiol.* **91**, 561–570.

Marty A. (1981) Ca-dependent K channels with large unitary conductance in chromaffin cell membranes. *Nature* **291**, 497–500.

Marty A. and Neher E. (1985) Potassium channels in cultured bovine adrenal chromaffin cells. *J. Physiol.* **367**, 117–141.

Muraki K. and Imaizumi Y. (2001) A novel function of sphingosine-1-phosphate to activate a non-selective cation channel in human endothelial cells. *J. Physiol.* **537**, 431–441.

Nathan C. F. (1987) Secretory products of macrophages. *J. Clin. Invest.* **79**, 319–326.

Noh S. J., Kim M. J., Shim S. and Han J. K. (1998) Different signaling pathway between sphingosine-1-phosphate and lysophosphatidic acid in Xenopus oocytes: functional coupling of the sphingosine-1-phosphate receptor to PLC-xβ in Xenopus oocytes. *J. Cell Physiol.* **176**, 412–423.

Ohta T., Ito S. and Nakazato Y. (1998) Ca^{2+}-dependent K^+ currents induced by muscarinic receptor activation in guinea pig adrenal chromaffin cells. *J. Neurochem.* **70**, 1280–1288.

Okajima F. (2001) Establishment of the method for the measurement of sphingosine-1-phosphate in biological samples and its application for S1P research. *Nippon Yakurigaku Zasshi* **118**, 383–388.

Pan C. Y., Jeromin A., Lundstrom K., Yoo S. H., Roder J. and Fox A. P. (2002) Alterations in exocytosis induced by neuronal Ca^{2+} sensor-1 in bovine chromaffin cells. *J. Neurosci.* **22**, 2427–2433.

Pan C. Y., Lee H. and Chen C. L. (2006) Lysophospholipids elevate $[Ca^{2+}]_i$ and trigger exocytosis in bovine chromaffin cells. *Neuropharmacology* **51**, 18–26.

Panetti T. S. (2002) Differential effects of sphingosine 1-phosphate and lysophosphatidic acid on endothelial cells. *Biochim. Biophys. Acta* **1582**, 190–196.

Panetti T. S., Magnusson M. K., Peyruchaud O., Zhang Q., Cooke M. E., Sakai T. and Mosher D. F. (2001) Modulation of cell interactions with extracellular matrix by lysophosphatidic acid and sphingosine 1-phosphate. *Prostaglandins Other Lipid Mediat.* **64**, 93–106.

Prakriya M., Solaro C. R. and Lingle C. J. (1996) $[Ca^{2+}]_i$ elevations detected by BK channels during Ca^{2+} influx and muscarine-mediated release of Ca^{2+} from intracellular stores in rat chromaffin cells. *J. Neurosci.* **16**, 4344–4359.

Rosen H. and Goetzl E. J. (2005) Sphingosine 1-phosphate and its receptors: an autocrine and paracrine network. *Nat. Rev. Immunol.* **5**, 560–570.

Schilling T., Stock C., Schwab A. and Eder C. (2004) Functional importance of Ca^{2+}-activated K^+ channels for lysophosphatidic acid-induced microglial migration. *Eur. J. Neurosci.* **19**, 1469–1474.

Schober A., Huber K., Fey J. and Unsicker K. (1998) Distinct populations of macrophages in the adult rat adrenal gland: a subpopulation with neurotrophin-4-like immunoreactivity. *Cell Tissue Res.* **291**, 365–373.

Schweizer F. E. and Ryan T. A. (2006) The synaptic vesicle: cycle of exocytosis and endocytosis. *Curr. Opin. Neurobiol.* **16**, 298–304.

Seung Lee W., Hong M. P., Hoon Kim T., Kyoo Shin Y., Soo Lee C., Park M. and Song J. H. (2005) Effects of lysophosphatidic acid on sodium currents in rat dorsal root ganglion neurons. *Brain Res.* **1035**, 100–104.

Smith C. and Neher E. (1997) Multiple forms of endocytosis in bovine adrenal chromaffin cells. *J. Cell Biol.* **139**, 885–894.

Taha T. A., Argraves K. M. and Obeid L. M. (2004) Sphingosine-1-phosphate receptors: receptor specificity versus functional redundancy. *Biochim. Biophys. Acta* **1682**, 48–55.

Wang J., Carbone L. D. and Watsky M. A. (2002) Receptor-mediated activation of a Cl^- current by LPA and S1P in cultured corneal keratocytes. *Invest. Ophthalmol. Vis. Sci.* **43**, 3202–3208.

Winkler H. (1993) The adrenal chromaffin granule: a model for large dense core vesicles of endocrine and nervous tissue. *J. Anat.* **183**, 237–252.

Wu S. N., Lo Y. K., Li H. F. and Shen A. Y. (2001) Functional coupling of voltage-dependent L-type Ca^{2+} current to Ca^{2+}-activated K^+ current in pituitary GH3 cells. *Chin. J. Physiol.* **44**, 161–167.

Xiao Y., Chen Y., Kennedy A. W., Belinson J. and Xu Y. (2000) Evaluation of plasma lysophospholipids for diagnostic significance using electrospray ionization mass spectrometry (ESI-MS) analyses. *Ann. NY Acad. Sci.* **905**, 242–259.

Xu Y. J., Aziz O. A., Bhugra P., Arneja A. S., Mendis M. R. and Dhalla N. S. (2003) Potential role of lysophosphatidic acid in hypertension and atherosclerosis. *Can. J. Cardiol.* **19**, 1525–1536.

Yatomi Y., Igarashi Y., Yang L., Hisano N., Qi R., Asazuma N., Satoh K., Ozaki Y. and Kume S. (1997) Sphingosine 1-phosphate, a bioactive sphingolipid abundantly stored in platelets, is a normal constituent of human plasma and serum. *J. Biochem. (Tokyo)* **121**, 969–973.

Yin F. and Watsky M. A. (2005) LPA and S1P increase corneal epithelial and endothelial cell transcellular resistance. *Invest. Ophthalmol. Vis. Sci.* **46**, 1927–1933.

Zhang Y., Fehrenbacher J. C., Vasko M. R. and Nicol G. D. (2006) Sphingosine-1-phosphate via activation of a G protein-coupled receptor(s) enhances the excitability of rat sensory neurons. *J. Neurophysiol.* **96**, 1042–1052.

出席
「First Asian Spectroscopy Conference & Asian Biospectroscopy Conference」
國際會議報告

國立臺灣大學化學系暨研究所

陳逸聰

一. 參加會議經過

First Asian Spectroscopy Conference & Asian Biospectroscopy Conference 於 2007 年 1 月 29 日至 2 月 2 日在 Bangalore, India 舉行，會議主題有傳統之光譜，但新趨勢為鼓勵往奈米材料及生化相關之光譜研究發展為目標。本人榮幸受邀在會議中演講（題目：Nanotubes and Nanowires Based Field Effect Transistors as Biological Sensors）。此外，本人此次亦帶一名學生李長琪前往參加，拓展學生之國際視野，學生之壁報（題目：Detection of Avian Influenza H5N2 Virus by Silicon Nanowire Field Effect Transistors）也已在大會上發表。

此次會議分為：Raman spectroscopy, High resolution & Gas-phase clusters, Theory of dynamics, Surface and thin films, Time-resolved spectroscopy, Ultrafast dynamics, Nanoparticles, Computational methods, UV/visible spectroscopy, New techniques, Bio-analytical methods, Spectroscopy in medicine, Bio-medical applications, Biospectroscopy, General spectroscopy 等近 20 個 divisions，共約 2 百多人參加，此外壁報展示活動亦分 3 天舉行。由於主辦之 Indian Institute of Science 為印度頂尖之高等研究學府，參與之教授與學生相當踴躍，為相當成功之一次國際光譜會議。

二. 與會心得

在會議中，我聽取了相當多場的演講，雖然皆與光譜研究相關，但以光譜方法結合奈米材料與生化醫學為應用的研究題材相當盛行。演講題材相當廣泛，彼此討論切磋，不失為一學術國際交流的好場合。尤其亞洲區域：包括台灣，日本，韓國，大陸，新加坡，澳洲，紐西蘭，印度等國家之相關研究人員參與熱烈，將來應會蔚成亞洲地區之重要會議。

在本人的演講中，我先以本實驗室近年來所完成之奈米材料光譜做為介紹，其中包括(1). Surface enhanced Raman scattering and polarized photoluminescence from catalytically grown CdSe nanobelts and sheets and (2). Photoluminescence and Raman Scattering from Catalytically Grown $Zn_xCd_{1-x}Se$ Alloy Nanowires。接著介紹最近我們利用單壁碳奈米管做成場效電晶體，並在碳奈米管上先化學修飾分子抗體，以做為神經細胞在受刺激後分泌出生化分子，我們便及時利用單壁碳奈米管場效電晶體來偵測此分泌出之生化分子（In-situ detection of chromogranin A released from living neurons with single-walled carbon nanotube field-effect transistor）。最後並強調這種奈米管（線）場效電晶體憑藉其非常靈敏，並可臨場與及時的偵測活細胞分泌之生化分子，將來必然在生化醫學上拌演重要角色，並在生化分析上做為研究各種生物及化學體系的新工具。

三. 攜回資料名稱及內容

帶回此次會議論文目錄及摘要一本，供有興趣者研讀。